International Journal of Psychophysiology 91 (2014) 104–120

Contents lists available at ScienceDirect

International Journal of Psychophysiology

journal homepage: www.elsevier.com/locate/ijpsycho

Auditory event-related potentials and alpha oscillations in the psychosis prodrome: Neuronal generator patterns during a novelty oddball task

Jürgen Kayser [a,b,*], Craig E. Tenke [a,b], Christopher J. Kroppmann [b], Daniel M. Alschuler [b], Shiva Fekri [b], Shelly Ben-David [b], Cheryl M. Corcoran [a,b], Gerard E. Bruder [a,b]

[a] Department of Psychiatry, Columbia University College of Physicians & Surgeons, New York, NY, USA
[b] Division of Cognitive Neuroscience, New York State Psychiatric Institute, New York, NY, USA

ARTICLE INFO

Article history:
Received 12 June 2013
Received in revised form 3 December 2013
Accepted 6 December 2013
Available online 13 December 2013

Keywords:
Event-Related Potentials (ERP)
Current Source Density (CSD)
Principal Components Analysis (PCA)
Novelty oddball
Mismatch Negativity (MMN)
Time–frequency analysis
Alpha ERD
Clinical High-Risk (CHR)

ABSTRACT

Prior research suggests that event-related potentials (ERP) obtained during active and passive auditory paradigms, which have demonstrated abnormal neurocognitive function in schizophrenia, may provide helpful tools in predicting transition to psychosis. In addition to ERP measures, reduced modulations of EEG alpha, reflecting top-down control required to inhibit irrelevant information, have revealed attentional deficits in schizophrenia and its prodromal stage. Employing a three-stimulus novelty oddball task, nose-referenced 48-channel ERPs were recorded from 22 clinical high-risk (CHR) patients and 20 healthy controls detecting target tones (12% probability, 500 Hz; button press) among nontargets (76%, 350 Hz) and novel sounds (12%). After current source density (CSD) transformation of EEG epochs (−200 to 1000 ms), event-related spectral perturbations were obtained for each site up to 30 Hz and 800 ms after stimulus onset, and simplified by unrestricted time–frequency (TF) principal components analysis (PCA). Alpha event-related desynchronization (ERD) as measured by TF factor 610–9 (spectral peak latency at 610 ms and 9 Hz; 31.9% variance) was prominent over right posterior regions for targets, and markedly reduced in CHR patients compared to controls, particularly in three patients who later developed psychosis. In contrast, low-frequency event-related synchronization (ERS) distinctly linked to novels (260–1; 16.0%; mid-frontal) and N1 sink across conditions (130–1; 3.4%; centro-temporoparietal) did not differ between groups. Analogous time-domain CSD-ERP measures (temporal PCA), consisting of N1 sink, novelty mismatch negativity (MMN), novelty vertex source, novelty P3, P3b, and frontal response negativity, were robust and closely comparable between groups. Novelty MMN at FCz was, however, absent in the three converters. In agreement with prior findings, alpha ERD and MMN may hold particular promise for predicting transition to psychosis among CHR patients.

1. Introduction

For most individuals affected by schizophrenia, the first onset of symptoms is preceded by a prodromal period characterized by attenuated psychotic symptoms, anxiety, social and role dysfunction, and affective symptoms (Häfner et al., 2003). Early recognition of individuals who later develop psychosis holds the promise of preventing or delaying onset through early intervention (e.g., Corcoran et al., 2010). However, despite considerable efforts in studying individuals at clinical high risk (CHR) for psychosis (see Fusar-Poli et al., 2013, for a recent review), little is known about the underlying pathophysiology of emerging psychosis.

1.1. Neurophysiologic abnormalities in the psychosis prodrome

A multitude of neurophysiologic abnormalities have been documented in schizophrenia (e.g., Luck et al., 2011), some of which may potentially be used as translational biomarkers for drug discovery (e.g., Javitt et al., 2008). These abnormalities include electroencephalography (EEG) measures obtained in the time domain, notably event-related potentials (ERPs) that index neuronal functions ranging from early sensory (e.g., P1, N1) to late cognitive (e.g., P3) processing, or in the frequency domain, including power spectra that index attentional control (e.g., alpha) or binding of perceptual features (e.g., gamma). Initially, high expectations had been placed in the almost ubiquitous reduction of P3 amplitude, which has been associated with negative symptoms and may serve both as a state and trait marker of schizophrenia (e.g., Mathalon et al., 2000); however, a decrease in P3 amplitude is not specific to the disorder and is often observed, for example, in alcoholism, depression, bipolar disorder, or Alzheimer's disease (e.g., Ford, 1999). Still, P3 reductions and other neurophysiologic deficits have also been observed in unaffected relatives and first-episode patients

* Corresponding author at: New York State Psychiatric Institute, Division of Cognitive Neuroscience, Unit 50, 1051 Riverside Drive, New York, NY 10032, USA. Tel.: +1 646 774 5207; fax: +1 212 543 6540.
E-mail address: kayserj@nyspi.columbia.edu (J. Kayser).

0167-8760/$ – see front matter © 2013 Elsevier B.V. All rights reserved.
http://dx.doi.org/10.1016/j.ijpsycho.2013.12.003

(e.g., Bramon et al., 2005; Ford, 1999; Hirayasu et al., 1998; Michie, 2001; Turetsky et al., 2000; van der Stelt et al., 2005; Winterer et al., 2003), suggesting that certain electrophysiologic measures may be candidate risk biomarkers that may identify individuals at risk for schizophrenia (e.g., Luck et al., 2011).

A promising line of research has recently implicated various neurophysiologic measures obtained during active and passive *auditory* paradigms as potential tools in predicting transition to psychosis (Atkinson et al., 2012; Bodatsch et al., 2011; Frommann et al., 2008; Higuchi et al., 2013; Jahshan et al., 2012; Koh et al., 2011; Murphy et al., 2013; Shaikh et al., 2012; van der Stelt et al., 2005; van Tricht et al., 2010). Interestingly, while cognitive impairments in schizophrenia are typically studied with visual paradigms (e.g., Barch and Smith, 2008; Barch et al., 2009, 2012), neurophysiologic abnormalities are often more common or more pronounced in the auditory than visual modality (e.g., Egan et al., 1994; Ford et al., 1994; Ford, 1999; Kayser et al., 2009; Pfefferbaum et al., 1989). Deficits in auditory mismatch negativity (MMN), a preattentive measure of auditory change detection, have rather consistently been found in schizophrenia (e.g., Javitt et al., 2008; Michie, 2001), and this electrophysiologic measure has been considered a promising biomarker candidate to indicate transition to psychosis (e.g., Luck et al., 2011).

In one of the first neurophysiologic studies of psychosis risk, van der Stelt et al. (2005) employed an auditory target detection (oddball) task and found that CHR patients ($n = 10$) had reduced P3 amplitudes at parietal, centroparietal and central scalp sites when compared with age- and sex-matched controls. In other cross-sectional studies, Bramon et al. (2008) and Özgürdal et al. (2008) reported moderately reduced P3 in CHR patients ($n = 35$ and $n = 54$, respectively) when compared to controls, and Frommann et al. (2008) observed a widespread reduction of P3 in a large sample of CHR patients studied during an early ($n = 50$) or late ($n = 50$) initial prodromal state. In a longitudinal design, van Tricht et al. (2010) observed reduced target P3b in 18 CHR patients who later developed psychosis. Although none of these studies reported a reduction of auditory N1 amplitude in CHR patients, several cross-sectional studies observed reductions in MMN, showing that CHR individuals had reduced MMN amplitude to deviant tones differing from standard 1000-Hz tones in stimulus duration (Atkinson et al., 2012; Hsieh et al., 2012; Jahshan et al., 2012; Murphy et al., 2013; Shin et al., 2009). Studies that directly compared individuals with or without subsequent transition to psychosis found MMN reductions to be more severe or only present in those patients who later developed psychosis (Bodatsch et al., 2011; Higuchi et al., 2013; Shaikh et al., 2012). Brockhaus-Dumke et al. (2005) found only a non-significant MMN reduction in CHR patients, which was intermediate between controls and schizophrenia patients. As in schizophrenia, MMN deficits in CHR patients appear to be more robust for deviations in tone duration rather than pitch, and may also only be present in low but not high functioning patients (Hay et al., 2013).

Atkinson et al. (2012) also reported that an early P3 subcomponent with a frontocentral distribution, termed P3a, was reduced in CHR individuals, but this deficit was unrelated to MMN reductions. Reduced amplitudes of duration MMN and P3a have also been found in 17 first-episode patients, underscoring the potential phenotype value of both EEG measures (Hermens et al., 2010). Of interest, Salisbury et al. (2002) found reduced MMN to deviations in pitch for chronic schizophrenia ($n = 16$) but not for 21 first-episode patients, suggesting that MMN to deviations of tone duration reflect different aspects of neurophysiological processing. Notably, most of this ERP research in schizophrenia and CHR patients has relied on standard two-tone paradigms, but P3a is particularly evident to perceptually novel distractors embedded in a series of frequent nontarget and infrequent target stimuli, and has therefore been termed novelty P3 (Polich, 2007). In such a three-stimulus oddball task (Friedman et al., 1993), novelty P3 and P3b can be readily distinguished by their topographic differences (mid-frontocentral vs. mid-parietal maximum) *and* condition dependencies. Although a novelty oddball paradigm has previously been employed in schizophrenia using ERP (e.g., Mathalon et al., 2010) or functional magnetic resonance imaging (fMRI) measures (e.g., Laurens et al., 2005), with the former study failing to observe differential deficits of P3a and P3b and the latter suggesting that patients less efficiently divide processing resources between detecting and responding to the task-relevant target tones and reorienting and ignoring task-irrelevant novel sounds, to our knowledge, there are no such studies involving CHR patients.

In recent years, there has also been an increasing interest in abnormal neural oscillations in schizophrenia (e.g., Uhlhaas et al., 2008; Uhlhaas and Singer, 2010). Stimulus-induced or event-related changes in ongoing rhythmic EEG activity substantially contribute to the observed ERP components (e.g., Gruber et al., 2005; Makeig et al., 2002; Sauseng et al., 2007). Neurophysiologic techniques involving EEG or magnetoencephalography (MEG) provide high-temporal resolution and are therefore ideal for assessing oscillatory activation. However, the averaging process underlying ERPs generally prevents the study of neural oscillations (e.g., Pfurtscheller and Lopes da Silva, 1999). Several spectral decomposition approaches allow the study of event-related EEG oscillations that are poorly represented or absent in ERPs (e.g., Roach and Mathalon, 2008, for a review). Most of the time–frequency EEG research in schizophrenia has focused on high-frequency (i.e., beta and gamma) modulations (e.g., Ford et al., 2008; Spencer et al., 2003, 2004; Uhlhaas and Singer, 2010). Nonetheless, low-frequency modulations involving alpha and theta bands are associated with working memory, attention, inhibition and top-down cognitive control (Uhlhaas and Singer, 2010, for a review), functional domains that are the hallmark of cognitive impairments in schizophrenia (e.g., Barch and Smith, 2008).

Few studies in schizophrenia and individuals at risk have investigated reductions of alpha or theta activity as a function of cognitive performance. Among them, Higashima et al. (2007), using an auditory oddball paradigm, found that healthy controls showed a relative reduction in alpha power to targets compared with nontargets that was markedly reduced in schizophrenia patients. This reduction was unrelated to the observed reduction of P3 amplitude in patients, suggesting that alpha desynchronization indexes a different aspect of cognitive processing. More recently, a magnetoencephalography study by Koh et al. (2011) reported diminished alpha event-related desynchronization to target tones in 17 CHR individuals, which was intermediate between that of schizophrenia patients ($n = 10$) and healthy controls ($n = 18$).

1.2. The present study

Given prior evidence of P3a and/or P3b (e.g., Atkinson et al., 2012; Frommann et al., 2008) and alpha event-related desynchronization (Koh et al., 2011) abnormalities in CHR patients, we sought to study these time and time–frequency measures concurrently in a novelty oddball paradigm (Bruder et al., 2009). We employed a generic strategy for ERP analysis, which combines current source density (CSD) transformations of surface potentials with principal components analysis (PCA) to yield data-driven and physiologically-meaningful component estimates (e.g., Kayser and Tenke, 2003, 2006a, 2006b). This approach improves on conventional ERP analysis by obtaining unique ERP component measures that are independent of the EEG recording reference (cf. Kayser and Tenke, 2010), while also having an unambiguous polarity and sharper topography (Tenke and Kayser, 2012). This approach also addresses the spatial smearing of the EEG at scalp by volume conduction, which may lead to spurious EEG coherence (e.g., Fein et al., 1988; Guevara et al., 2005; Roach and Mathalon, 2008; Schiff, 2005), although these issues have an even wider impact on EEG spectral analysis (cf. Fig. 1 in Tenke and Kayser, 2005). For these reasons, the present study extends the temporal (e.g., Kayser and Tenke, 2006a) and frequency (e.g., Tenke and Kayser, 2005) CSD-PCA approach to time–frequency EEG analysis in an effort to confirm the MEG findings of Koh et al. (2011), which are also, by virtue of the imaging technique, unaffected

by choice of EEG reference. However, given that our a priori hypotheses concerned alpha desynchronization, the present time–frequency analysis was restricted to low-frequency components characterizing alpha or theta, despite the ability of this unbiased, data-driven approach to concisely summarize any spectral activation pattern within the time–frequency data space.

Specifically, we hypothesized that target and novelty P3, as well as alpha event-related desynchronization following P3, would be reduced in CHR patients. While target and novelty P3 are typically observed with ERPs during a novelty oddball (e.g., Bruder et al., 2009), the CSD transform also reveals a distinct component complex that uniquely characterizes the brain's response to novel stimuli, which is obscured by volume-conducted surface potentials (Tenke et al., 2010). This sink/source complex consists of a robust vertex-maximum source with an approximate peak latency of 250 ms that we termed novelty vertex source (NVS), which is preceded by a marked negativity that we originally termed novelty N2 sink (180 ms peak latency, FCz maximum). To the extent that the NVS is linked to P3a, we also expected NVS reductions comparable to previous findings of reduced P3a in CHR patients (e.g., Atkinson et al., 2012; Hermens et al., 2010). Likewise, to the extent that the preceding novelty N2 sink is related to MMN, we anticipated deficits in novelty MMN in CHR patients. A secondary focus was whether these electrophysiologic measures may be of value for predicting transition to schizophrenia in CHR patients (e.g., Luck et al., 2011; Bodatsch et al., 2011; Higuchi et al., 2013; Shaikh et al., 2012; van Tricht et al., 2010).

2. Material and methods

2.1. Participants

The current protocol followed an odor detection task (Kayser et al., 2013) as part of a larger ERP study, with a substantial overlap of both samples (i.e., 20 CHR patients and 19 healthy participants provided valid data in both paradigms). After excluding the data of 1 patient and 1 control due to technical issues during the EEG recordings, the current sample included 22 CHR patients (15 male, 7 female) who were recruited from the *Center of Prevention & Evaluation* (COPE) at New York State Psychiatric Institute (NYSPI) at Columbia University. As a clinical research program, COPE evaluates and treats individuals aged between 12 and 30 years who are considered at heightened clinical risk for psychosis on the basis of attenuated psychotic symptoms and/or genetic risk in the context of functional decline, and follows the individuals for up to four years to determine transition to psychotic disorder, typically schizophrenia. As a control group, 20 healthy volunteers (13 male, 7 female) were recruited from the same source population in the New York metropolitan area. All participants received US$10/h plus an extra US$10 travel compensation for each research appointment.

Table 1 summarizes the demographic and clinical characteristics of CHR patients and healthy controls. The two groups did not differ in age (median 21.5 years), education (median 14 years), degree of right-handedness (median laterality quotient 87.5; Oldfield, 1971), or gender composition. All participants had no history of neurological illness or substance abuse and were ascertained with the *Structured Interview for Prodromal Syndromes* and *Scale of Prodromal Symptoms* (SIPS/SOPS; Miller et al., 2003). The inclusion/exclusion criteria were highly comparable to those described by Piskulic et al. (2012), including: 1) meeting criteria for at least one of three prodromal syndromes using the SIPS/SOPS; 2) no current or lifetime Axis I psychotic disorder; 3) intelligence quotient (Wechsler scales for children or adults) greater than 70; and 4) no current or past CNS disorder (medical or psychiatric) which may account for prodromal symptoms. As expected, CHR patients showed robust differences to healthy controls in all SOPS subscales (cf. Table 1), but there were no group × gender interactions or gender main effects.

The ethnic composition in both groups was representative for the New York region, including 17 Caucasian, 12 African–American, 2 Asian, and 11 individuals of more than one or unknown racial origin. The experimental protocol had been approved by the institutional review board and was undertaken with the understanding and written consent of each participant.

The current sample included three CHR patients who developed threshold psychosis as determined during the prospective follow-up by the "Presence of Psychosis" criteria in the SIPS/SOPS (cf. Miller et al., 1999, 2003). These 'converters' (1 male, 2 female) were aged 16, 23 and 27 years and had 10, 14 and 17 years of education, respectively. Their SIPS/SOPS scores ($M \pm SD$, positive, 9.3 ± 5.0; negative, 19.0 ± 6.9; disorganization, 9.3 ± 4.0; general, 12.0 ± 1.7; global assessment of function, 40.3 ± 2.1) were largely comparable to the overall patient sample (Table 1), although converters tended to show more negative symptoms. Because findings for these CHR individuals are of particular importance for determining whether electrophysiologic measures during auditory target detection have predictive value for transition to psychosis, descriptive summaries of their data are also separately reported when appropriate below.

2.2. Stimuli and procedure

The study employed a novelty oddball task (Friedman et al., 1993; Fabiani and Friedman, 1995) as detailed in two previous reports (Bruder et al., 2009; Tenke et al., 2010) using sounds developed at the Cognitive Electrophysiology Laboratory at NYSPI (Fabiani et al., 1996). Briefly, nontarget and target tones (300 ms duration, 350 Hz and

Table 1
Means, standard deviations (*SD*), and ranges for demographic and clinical variables.

	Prodromal patients (n = 22; 7 female)			Healthy controls (n = 20; 7 female)				
Variable	Mean	*SD*	Range	Mean	*SD*	Range	*F*	*p*
Age (years)	21.5	3.6	13–27	21.7	3.3	16–27		
Education (years)	13.7	2.2	9–18	14.4	1.8	12–18		
Handedness (LQ)[a]	68.9[b]	34.6	−40–100	79.4[c]	49.3	−100–100		
SOPS positive[d]	11.3	4.3	4–20	0.6	0.8	0–2	98.1	<.0001
SOPS negative[d]	12.5	6.0	3–27	1.1	1.7	0–6	53.5	<.0001
SOPS disorganization[d]	6.8	3.3	1–14	0.3	0.7	0–2	60.7	<.0001
SOPS general[d]	8.1	4.2	0–14	0.5	1.1	0–4	63.5	<.0001
SOPS modified GAF[d]	46.8	6.4	38–60	83.8	7.0	68–95	279.9	<.0001

Note. Only *F* ratios with $p < .10$ are detailed ($df = 1, 38$).
[a] Laterality quotient (Oldfield, 1971) can vary between −100.0 (completely left-handed) and +100.0 (completely right-handed).
[b] $n = 19$.
[c] $n = 16$.
[d] *Structured Interview for Prodromal Syndromes/Scale of Prodromal Symptoms* (SIPS/SOPS; Miller et al., 2003) subscales (possible range): positive symptoms (0–30); negative symptoms (0–36); disorganization symptoms (0–24); general symptoms (0–24); modified global assessment of function score (0–100).

500 Hz frequency, 76% and 12% probability) interspersed with unique novel sounds (e.g., animals, musical instruments, etc.; 100–400 ms duration, 12% probability) were presented binaurally over headphones at 85 dB SPL in pseudorandom order (1000 ms stimulus onset asynchrony). A total of 400 trials were distributed over 8 blocks of 50 trials, each block consisting of 38 nontargets, 6 targets, and 6 novels. Participants were seated in a sound-attenuated booth and instructed to keep their eyes on a fixation cross during the task and to press a button as quickly as possible when, and only when, they heard the target tone. Response hand was counterbalanced across blocks. Participants were not informed about the novel sounds, and if they asked questions about their presence, they were reminded to respond only to the target tones.

2.3. Data acquisition, recording, and artifact procedures

EEG recording procedures are detailed in Kayser et al. (2013). Briefly, using NeuroScan software (NeuroScan, 1993), continuous EEGs were acquired at 200 samples/s with a 48-channel Grass Neurodata recording system for an expanded 10–20 system scalp montage (Pivik et al., 1993; Jurcak et al., 2007), using a nose tip reference and analog hardware settings of 10 k gain and .01–30 Hz (−6 dB/octave) band pass. Volume-conducted blink artifacts were removed from the raw EEG by spatial singular value decomposition (NeuroScan, 2003). Recording epochs of 1200 ms (200 ms prestimulus baseline) were extracted offline, tagged for A/D saturation, and digitally low-pass filtered at 50 Hz (−24 dB/octave) to remove any residual high frequency activity from the EEG that is not relevant to ERPs, including digitizer noise. Using a reference-free approach to identify residual artifacts on a channel-by-channel and trial-by-trial basis (Kayser and Tenke, 2006d), artifactual surface potentials were either replaced by spherical spline interpolation (Perrin et al., 1989) using the data from artifact-free channels (i.e., when less than 25% of all EEG channels contained an artifact) or the affected trial was rejected.

Separate ERPs for nontarget, target and novel stimuli were averaged from artifact-free trials. The means for the number of trials ($\pm SD$) used to compute these ERP averages were 250.1 ± 31.7, 38.8 ± 5.6 and 34.9 ± 6.3 (nontarget, target and novel, respectively) for CHR patients, and 265.1 ± 16.6, 39.3 ± 2.6 and 36.6 ± 4.7 for healthy controls (no fewer than 20 trials per ERP), and there were no significant differences between patients and controls, $F(1, 38) = 2.55$, $p = .12$. Furthermore, a satisfactory signal-to-noise ratio for each condition was confirmed by visual inspections of the individual ERP waveforms of each participant. ERP waveforms were screened for electrolyte bridges (Tenke and Kayser, 2001),[1] low-pass filtered at 12.5 Hz (−12 dB/octave), and baseline-corrected using the 100 ms preceding stimulus onset.

2.4. Current source density, time–frequency analysis, and principal components analysis

As in our previous study (Tenke et al., 2010), ERP waveforms were transformed into CSD estimates (μV/cm^2 units; 10 cm head radius; 50 iterations; m = 4; smoothing constant $\lambda = 10^{-5}$) using a spherical spline surface Laplacian (Perrin et al., 1989; Kayser and Tenke, 2006a, 2006b; Kayser, 2009). For the time–frequency analyses of these data, the same transform was also applied to the single-trial EEG epochs used to compute these ERPs (averaging the CSD-transformed EEG epochs will yield identical CSD averages).

All time-locked CSD epochs for each participant and condition were imported into EEGlab (version 11.0.3.1b; Delorme and Makeig, 2004) to generate normalized time–frequency averages (function *timef.m*). Event-related spectral perturbations (ERSP; Makeig, 1993) were obtained by computing overall fast Fourier transform (FFT) power spectra (zero-padding ratio of 8) relative to the pre-stimulus baseline. Relative increases (synchronization; ERS) and decreases (desynchronization; ERD) in event-related spectral power were quantified by the $\log_{10}$-transformed ratio of overall power and baseline power (multiplied by 10), yielding normalized ERS/ERD measures (i.e., positive or negative values) for 128 spectral frequencies (0.78125 to 100 Hz) at 200 time points (−122.5 ms to 922.5 ms) for each participant, condition, and recording site. Note that the length for the moving subwindow was set to 32 samples (2^5 = 160 ms) and padded with zeros to yield 256 samples (32 * 8), which determined both the FFT frequency resolution (sampling frequency/number of samples = 200/256 = 0.78125) and the resulting ERSP time interval (epoch start + subwindow length/2 … epoch end subwindow length/2 = −200 + 80 … 1000–80 = −120 … 920 ms). These frequency-by-time (128-by-200) matrices were reduced via bilinear interpolation (Matlab function *interp2.m*) to 30-by-82 matrices to directly reflect spectral (1 to 30 Hz in steps of 1 Hz) and temporal (−10 to 800 ms in steps of 10 ms) ranges of interest.

To determine their common sources of variance, CSD waveforms were submitted to temporal PCA derived from the covariance matrix, followed by unrestricted Varimax rotation of the covariance loadings (Kayser and Tenke, 2003, 2006c). Using a MatLab function (appendix of Kayser and Tenke, 2003)[2] that emulates BMDP-4M algorithms (Dixon, 1992), a temporal PCA was computed using 221 variables (time interval −100 to 1000 ms) and 6174 observations stemming from 42 participants, 3 conditions, and 49 electrode sites. A similar approach successfully determined the common sources of variance underlying the time–frequency CSD (cf. Tenke et al., 2012).[3] Each 30-by-82 matrix was rearranged as a vector by concatenating the time vectors for each frequency, yielding a time–frequency vector of 2460 ERD/ERS values. Using the same Matlab function (appendix of Kayser and Tenke, 2003), these data (i.e., 2460 variables for 6174 observations) were then submitted to unrestricted time–frequency PCA, using the covariance matrix for factorization and Varimax rotation of the covariance loadings.[4]

[1] While no electrolyte bridges were detected in the current data set, thereby safeguarding against artifactual distortions in EEG topography that may affect ERP and ERSP measures and their CSD counterparts, a recent survey of publicly-available EEG data suggested that the problem is more widespread than commonly thought (Alschuler et al., 2013). Routine screening for electrolyte bridges will allow investigators to recognize any affected channels and treat these artifacts accordingly (e.g., by replacing the data via interpolation).

[2] The generic Matlab code can also be retrieved at URL http://psychophysiology.cpmc.columbia.edu/erpPCA.html.

[3] The common practice to extract temporal and spectral PCA factors across variance stemming from participants, conditions, and electrodes, using time (temporal) or frequency (spectral) values as variables, which is adopted here to expand the temporal and spectral ERP/EEG component concept (e.g., Donchin et al., 1977; Kayser and Tenke, 2003, 2005; Picton et al., 2000; Tenke and Kayser, 2005; van Boxtel, 1998) to time-frequency data, was criticized during the peer review of this article. Instead, it was suggested that submitting data from a single condition, and even a single location, may be more informative with regard to understanding the underlying neurophysiological mechanisms. However, when eliminating condition and topography, only the between-subjects variance will contribute to the extraction of a factor, which is incompatible with the intended quantification of the ERP/EEG component construct. Further, because a covariance association matrix removes the grand mean from the data, therefore factoring only the variance around the grand mean, the underlying neuronal generator activity may be completely obscured if the component of interest is equally present across individuals (i.e., the extracted factors will not represent the targeted variance).

[4] Although it is commonly recommended that the number of observations should be several times the number of variables (i.e., a ratio of no less than 5:1) to obtain a stable PCA solution (e.g., Bernat et al., 2005; Chapman and McCrary, 1995; Guadagnoli and Velicer, 1988), this convention does not take the highly-intercorrelated nature of EEG time series data into account, which renders adjacent variables (in time and/or frequency) highly redundant. We have previously found that even substantial deviations from this rule are not a problem when using unrestricted solutions for temporal PCA (Kayser and Tenke, 2003; Kayser et al., 2006), and this applies likewise to unrestricted frequency PCA (Tenke and Kayser, 2005; Tenke et al., 2011). To confirm that these considerations also hold for unrestricted time-frequency PCA, we compared the present tfPCA solution to those obtained for ERSP data matrices systematically reduced to ¼ of the variables (615), thereby changing the ratio of observations to variables from about 2.5:1 to about 10:1. The first 10 factors extracted in each of these four additional tfPCA solutions were virtually identical to the first 10 factors of the original tfPCA solution, indicating that the unrestricted tfPCA solution reported here was stable and not affected by the 2.5:1 ratio of observations to variables.

To interpret the resulting factors, their loading vectors were restored to 30-by-82 matrices to create conventional time–frequency plots. This approach, which is akin to the joint (simultaneous) extraction of stimulus- and response-locked components in the time domain (cf. Kayser et al., 2007), was preferred to a multiple-stage simplification (i.e., time and frequency) because of its simplicity and ease of interpretation, recognizing the ability of PCA to identify spectral and/or temporal processes that belong together. Similarly, noting that the specific sequence or order of variables is irrelevant for the PCA decomposition (e.g., Kayser and Tenke, 2003), Bernat et al. (2005) applied this strategy to time–frequency matrices, likewise producing factors from the vectorized matrices and, after factor restriction (Scree criterion), converting the rotated factor loadings vectors back to time–frequency matrices for easy interpretation. However, their study employed field potentials for a comparison of spectra derived from wavelets or reduced interference distributions, in contrasts to the present FFT-based ERSPs derived from CSDs. By virtue of the reference-independent Laplacian transform (see Tenke and Kayser, 2012, for a review), both the temporal (tPCA) and the time–frequency CSD factors (tfPCA) are associated with factor scores that directly reflect neuronal generator patterns at scalp. In striking contrast to surface potentials, however, CSD-PCA factors do not suffer from the interpretational ambiguity (i.e., signal location, polarity, or phase) stemming from the choice of EEG reference (e.g., Kayser and Tenke, 2010), a problem that is compounded by spectral analysis (i.e., non-linear data transformations; cf. Tenke and Kayser, 2005) and, by extension, time–frequency analysis (e.g., cf. Fein et al., 1988; Guevara et al., 2005; Schiff, 2005).

2.5. Statistical analysis

For the time domain, tPCA factor scores corresponding to CSD components previously identified for this novelty oddball paradigm (Tenke et al., 2010) were submitted to repeated measures ANOVAs with *group* (patients, controls) and *gender* (male, female) as between-subjects factors, and *condition* (target, novel) as a within-subjects factor (for the sake of simplicity and to increase statistical power, nontarget stimuli were not included in these analyses). The selection of recording sites for comparing experimental effects in these ANOVAs was guided by our previous findings using a 67-channel EEG montage (Tenke et al., 2010), and consisted of either midline sites or lateral, homologous recording sites over both hemispheres, and thereby adding either *site*, or *site* and *hemisphere* as within-subjects factors to the design. However, because recording sites were selected on the premise that they collectively represent sink or source activity associated with a given CSD component, site effects were not further pursued in these analyses. For the time–frequency domain, tfPCA factor scores corresponding to CSD-ERSP components unambiguously related to alpha ERS or alpha ERD were submitted to similar repeated measures ANOVAs, selecting subsets of recording sites at which tfPCA factor scores were largest and most representative of the associated CSD-ERSP component (cf. Kayser and Tenke, 2006a).

For analyses of the behavioral data, percentages of correct responses (button press to targets, no press to novels) were submitted to repeated measures ANOVA with *condition* as within-subjects factor, and *group* and *gender* as between-subjects factors. A *d′*-like sensitivity measure d_L (logistic distribution; Snodgrass and Corwin, 1988) was calculated from the hit rates for targets and the false alarm rates for novels and submitted to a two-way ANOVA with *group* and *gender*. This ANOVA design was also used for the mean latency of correct responses to targets.

Because the sample included almost twice as many male than female participants in each group, gender was only considered as a control factor in all statistical analyses. Simple effects (BMDP-4V; Dixon, 1992) provided a systematic means to examine sources of interactions. A conventional significance level ($p < .05$) was applied for all effects.

Pearson's correlations were used to evaluate associations between the electrophysiological measures (i.e., time vs. time–frequency domain) separately for each group. For patients only, the clinical variables were also correlated with the electrophysiological measures. Given our a priori hypotheses about the direction of these associations (i.e., greater severity of symptoms coupled with reduced CSD amplitudes), one-tailed significance levels are reported for these analyses.

3. Results

3.1. Behavioral data

Participants performed well on this task (Table 2). Whereas a false alarm rate of about 10% to novels was observed in both groups, performance to targets (button press) and nontargets (correct reject) was almost perfect, yielding high sensitivity values. The mean response latency for correct button presses to targets was about 30 ms slower in CHR patients compared to healthy controls. However, there were no significant group differences in any of these performance measures (all $F[1,38] \leq 2.54$, all $p \geq .12$).

The three converters tended to have poorer performance to targets and novels (nontarget = 99.8 ± 0.4; target = 93.7 ± 6.3; novel = 81.3 ± 21.2; $d_L = 5.22 \pm 3.43$) and slower (RT = 540.3 ± 82.0) but still adequate performance.

3.2. Electrophysiologic data

3.2.1. Time domain

Figs. 1 and 2 show the grand mean CSD waveforms separately for patients and controls, comparing differences between conditions. Fig. 3 directly compares the CSD waveforms of both groups for target and novel stimuli at selected midline sites. In close agreement with our previous findings for this novelty oddball paradigm (Tenke et al., 2010), N1 sinks peaking at about 135 ms over medial–central sites (C3/4) were followed by temporal N1 sinks (170 ms, T7/8) in all conditions. A novelty vertex source (NVS; 270 ms, Cz) was exclusively observed for novel stimuli. In contrast, a P3b source (380 ms, Pz) was most prominent for target stimuli, as was a response-related mid-frontal sink (FRN; 540 ms, Fz; cf. Kayser and Tenke, 2006a; Kayser et al., 2007).[5] The morphology of this CSD component structure (i.e., sequence, timing and amplitudes) was highly comparable across groups.

Fig. 4 shows the time courses of factor loadings for the first six CSD factors extracted (91.7% explained variance after rotation)[6] and corresponding factor score topographies for five meaningful CSD components expected for each condition. Labels reflect the peak latency

Table 2
Behavioral data summary: Grand means (±*SD*).

	Correct responses [%]			Sensitivity [d_L]	Latency [ms]
Group	Nontarget	Target	Novel		
Patients	99.9 ±0.2	98.7 ±2.9	88.6 ±10.8	6.53 ±6.78	472.5 ±86.0
Controls	99.9 ±0.2	99.0 ±2.0	91.0 ±6.4	6.63 ±6.75	439.3 ±57.9

[5] The acronym FRN was intentionally selected by Kayser et al. (2007), who simultaneously extracted stimulus- and response-locked CSD activity, because of its topographic similarity with other response-locked components (i.e., error-related negativity [ERN/Ne], correct response negativity [CRN/Nc], feedback-related negativity [FRN]) that are likely related to performance monitoring and evaluation (e.g., Gehring and Knight, 2000; Hoffmann and Falkenstein, 2012; Vidal et al., 2000). Whereas the characteristic focal, mid-frontal negativity (maximum at FCz) is clearly observed in response-locked ERP and CSD waveforms, it is obscured by volume conduction in stimulus-locked ERPs; however, it can still be characterized as a unique component after CSD transformation (Kayser and Tenke, 2006a, 2006b).

[6] A total of 92 factors were extracted and rotated, with 84 explaining less than 1% variance.

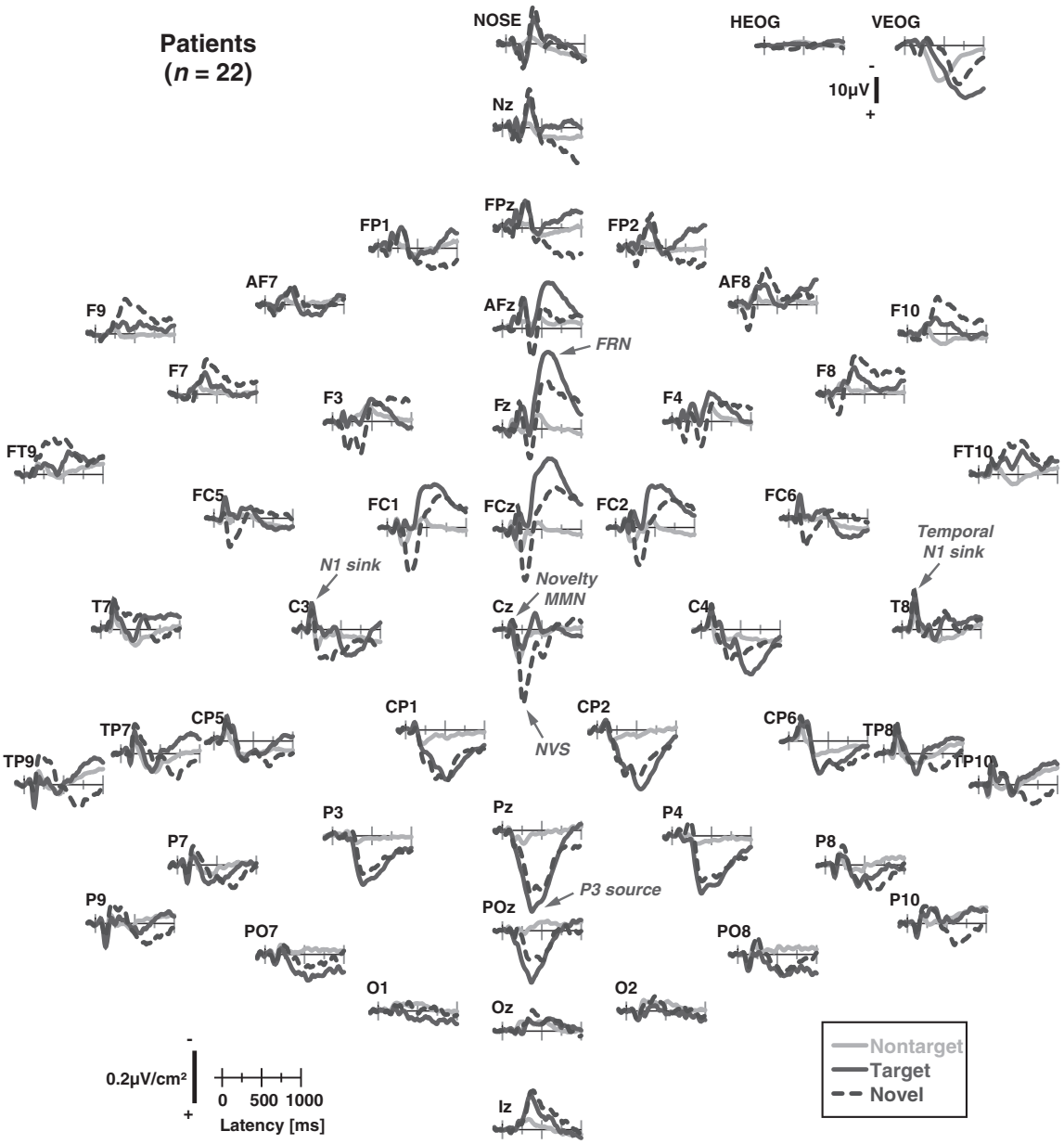

Fig. 1. Grand mean surface Laplacian (CSD) waveforms (−100 to 1000 ms, 100 ms pre-stimulus baseline) for 22 clinical high-risk patients comparing nontarget, target, and novel stimuli at all 49 recording sites. Horizontal and vertical electrooculograms (EOG) are shown before blink correction.

of the factor loadings relative to stimulus onset. The extracted factors closely paralleled those of Tenke et al. (2010). A characteristic auditory N1 sink dipole generator pattern spanning the Sylvian fissure (auditory cortex) was observed over each hemisphere (most prominent for targets and novels), which merged into a systematically delayed sink over temporal sites. This temporal N1 sink was accompanied by a mid-central P2 source for nontargets, and an additional focal sink at FCz for novels (novelty MMN or novelty N2 sink; cf. Tenke et al., 2010). A robust NVS (novels only) preceded a classical P3b source with a mid-parietal maximum for targets, which included a mid-frontal P3a source, particularly for novels. As expected, a distinct FRN was seen for targets, with a peak latency of about 50-ms after the mean response latency (Table 2; cf. Kayser et al., 2007). Finally, a high-variance factor (935), with a peak latency near the end of the recording epoch, accounted for unsystematic variance associated with the baseline correction procedure (Kayser and Tenke, 2003). Almost identical topographies were observed for CHR patients and healthy controls (see Supplementary Fig. S1).

The statistical analyses for these CSD components at selected regions are summarized in Table 3, confirming the observed differences between target and novel stimuli across groups (Fig. 4). N1 sink at medial frontocentral sites (−1.23 ± 0.99 vs. −1.00 ± 1.09) and temporal N1 sink at lateral–temporal sites (−0.91 ± 1.13 vs. −0.56 ± 1.29) were larger for target than novel stimuli. In contrast, novelty MMN (0.36 ± 0.91 vs. −0.86 ± 1.59) and NVS (0.31 ± 1.24 vs. 1.58 ± 2.04) at mid frontocentral sites were effectively present for novel sounds but not for target tones (see also Fig. 3). Likewise, the mid-frontocentral portion of factor 350 (P3a) was more robust for novel (1.00 ± 1.20) than target (0.39 ± 1.07) stimuli, whereas the mid-parietal portion of factor 350 (P3b) did not differ between these two conditions. Lastly, factor 505 revealed robust condition effects in favor of target compared to novel stimuli, with greater FRN sink at mid-frontal sites (−1.96 ± 1.24 vs. −1.11 ± 1.18) and greater FRN source at centroparietal sites (1.22 ± 1.03 vs. 0.67 ± 0.72).

Most importantly, these analyses revealed no significant group main effects, although there were three group × condition interactions

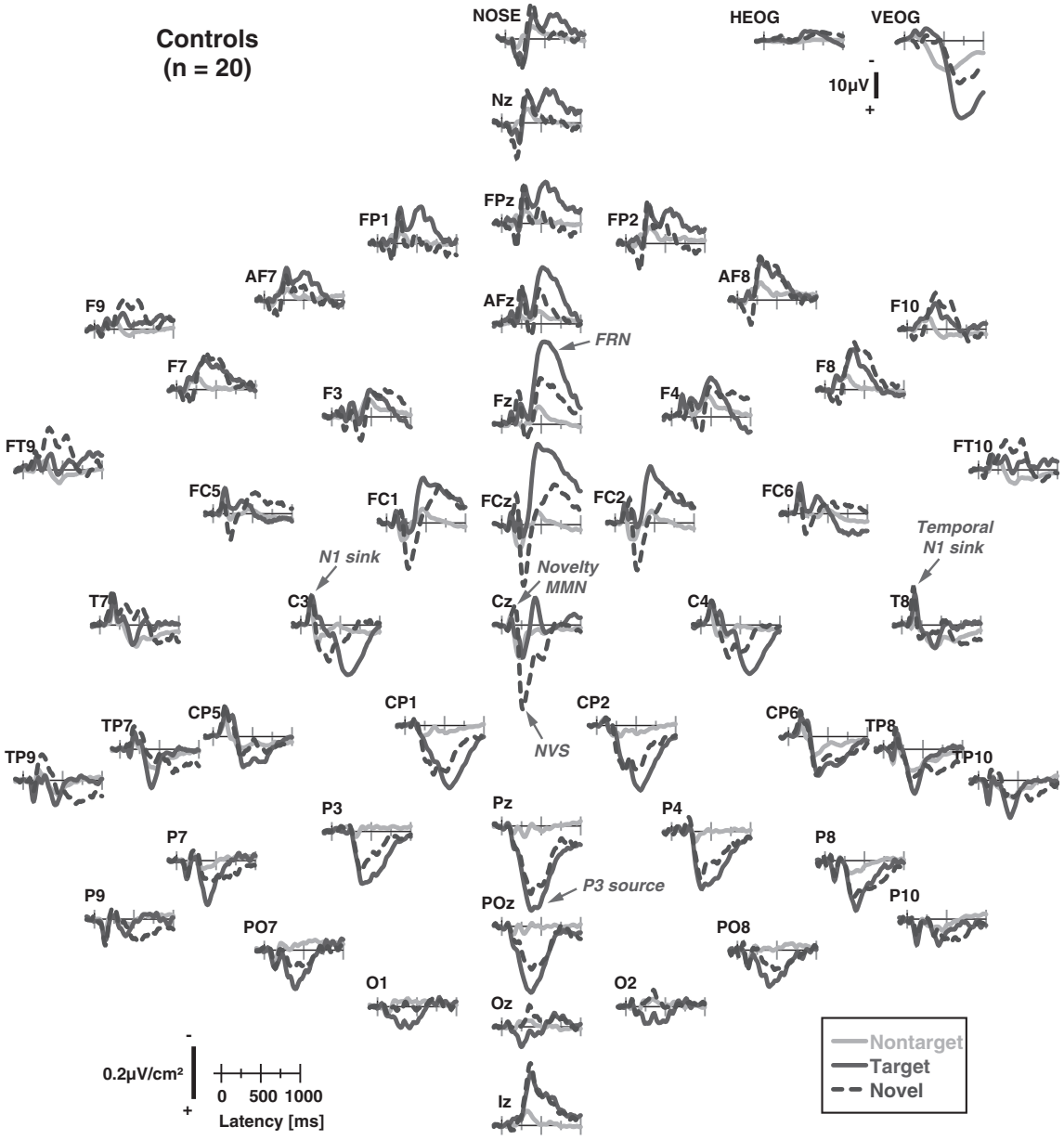

Fig. 2. CSD waveforms as in Fig. 1 for 20 healthy controls.

(Table 3). For the temporal N1 sink, the marginal significance for this two-way interaction stemmed from greater amplitudes for targets than novels in controls ($F[1,38] = 12.2$, $p = .001$) but not patients ($F[1,38] < 1.0$). Also for factor 185, the greater mid-frontal sink for novels than targets (novelty MMN) was less robust for patients ($F[1,38] = 9.66$, $p = .004$) than controls ($F[1,38] = 35.2$, $p < .0001$), but there were no significant simple effects of group for targets ($F[1,38] < 1.0$) or novels ($F[1,38] = 2.54$, $p = .12$). For the response-related centroparietal source (factor 505), simple effects of condition were less robust for patients ($F[1,38] = 5.10$, $p = .03$) than controls ($F[1,38] = 25.5$, $p < .0001$). This group × condition interaction was further modified by a significant three-way interaction involving hemisphere, which originated from right-greater-than-left hemisphere differences in controls for novels ($F[1,38] = 5.69$, $p = .02$) but not targets ($F[1,38] < 1.0$), whereas the same asymmetry was present in patients for targets ($F[1,38] = 5.65$, $p = .02$) but not novels ($F[1,38] = 1.63$, $p = .21$).

3.2.2. Time–frequency domain

Fig. 5 shows the grand mean CSD-ERSP plots, arranged as topographies, for patients and controls in each condition, while Fig. 6 shows enlarged CSD-ERSP plots at sites FCz (ERS maximum) and CP2 (ERD maximum) for target and novel stimuli. For both groups, prominent ERS effects for target and novel stimuli are clearly present between 100 and 400 ms for spectra between delta and alpha frequencies (1–10 Hz), being most robust over midfrontal regions, particularly for novels. This is followed by alpha ERD effects, maximum for target stimuli beyond 400 ms, covering posterior sites but being most robust over the right centroparietal region. These alpha ERD effects were markedly reduced in patients compared to controls. However, the basic morphology of the time–frequency CSD component structure (i.e., sequence and timing across conditions) was nevertheless highly comparable across groups.

Fig. 7 shows the time–frequency matrices of factor loadings and corresponding factor score topographies for three extracted CSD factors

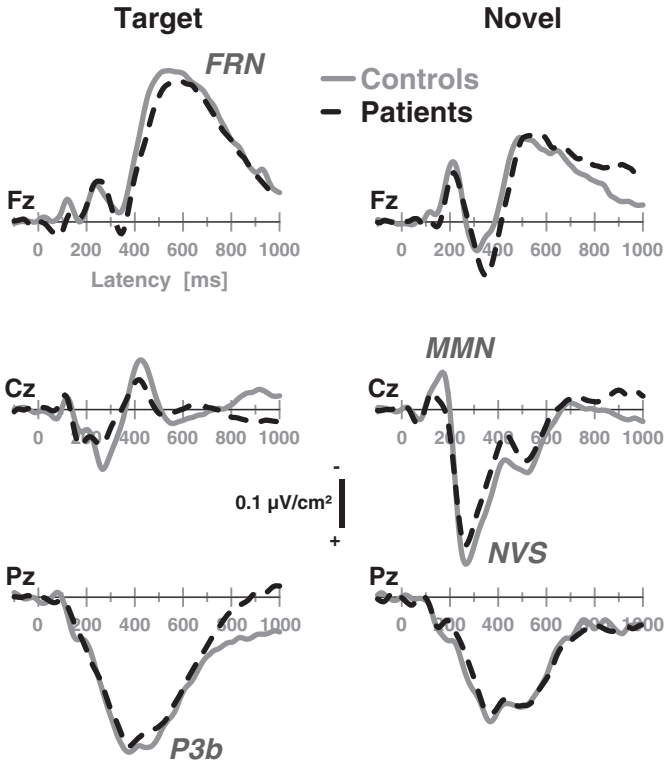

Fig. 3. CSD waveforms at selected midline sites (Fz, Cz, Pz) for target and novel stimuli comparing 22 patients and 20 controls. Three prominent CSD components are labeled for novels at site Cz (NVS: novelty vertex source) and for targets at sites Pz (P3b) and Fz (FRN: frontal response negativity).

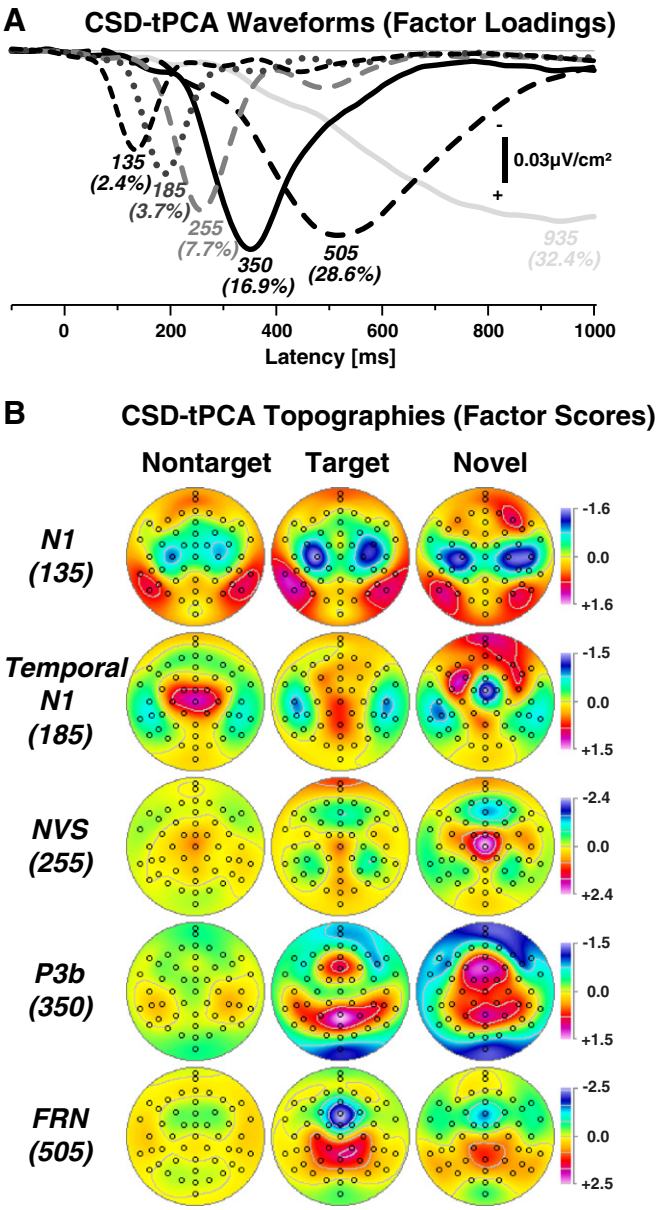

Fig. 4. (A) Factor loadings of the first six temporal PCA (tPCA) factors (with explained variance) extracted from the time-locked CSD waveforms ($N = 42$). Factor labels reflect the peak latency [ms] of the factor loadings. (B) CSD factor score topographies corresponding to N1 sink (135 ms peak latency of factor loading), temporal N1 sink (185 ms), novelty vertex source (NVS; 255 ms), P3b source (350 ms), and frontal response negativity (FRN; 505 ms) comparing nontarget, target and novel stimuli (pooled across all 42 participants; for separate topographies for each group, see Supplementary Fig. S1). All topographies are two-dimensional representations of spherical spline interpolations ($m = 2$; $\lambda = 0$) derived from the mean factors scores for each recording site.

(i.e., factors 1, 2 and 6; 51.4% explained variance after rotation) that reflected meaningful alpha ERSP (for additional beta ERSP factors, see Supplementary Fig. S2; for the loadings of 15 factors explaining at least 1% variance, see Supplementary Fig. S3).[7] In close analogy to the tPCA, factor labels were chosen to jointly reflect peak latency and frequency of the factor loadings. Similarly, the associated neuronal activation is inferred from the corresponding database, the time–frequency plots (Figs. 5 and 6), but the ERSP direction (i.e., ERS/ERD) is directly reflected by the sign of the factor scores. Note that, unlike Fig. 4B, the topographies of the tfPCA factors do not directly reflect sinks and sources but rather ERS and ERD activity derived from sink and source oscillations. The positive (red-purple) areas in the factor loadings plots (Fig. 7A) indicate the time–frequency range for a given factor, for example, spanning alpha to delta frequencies (spectral peak at 9 Hz) between 400 and 800 ms (temporal peak at 610 ms) for factor 610–9 (alpha ERD). The corresponding topographies reveal at which sites (scalp regions) factor scores are increased or decreased in relation to the grand mean (removed by factoring the covariance matrix), which translates into synchronization (ERS) or desynchronization (ERD). For the alpha ERD factor, the corresponding topographies for controls reveal little 'alpha ERD' (i.e., alpha to theta ERD between 400 and 800 ms) for nontargets across all sites (broad orange in Fig. 7B, row 2, column 1), prominent alpha ERD for targets over parietal, particular right parietal sites (blue areas in Fig. 7B, row 2, column 2), and less alpha ERD for novels over the same right parietal region (light blue areas in Fig. 7B, row 2, column 3). By comparison, alpha ERD was notably reduced in CHR patients (blue areas in Fig. 7B, row 1, columns 2 and 3). This pattern is entirely consistent which what can be seen from the original ERSP plot for each group, condition and site (Fig. 5), but the factor scores provide a superior summary measure for this activity.

[7] A total of 643 factors were extracted and rotated, with 628 explaining less than 1% variance.

Therefore, the first two factors clearly corresponded to the alpha ERD (factor 610–9) and the preceding ERS coincided with the NVS (factor 260–1). This interpretation was corroborated by the condition-dependent topographies, which revealed 1) a prominent ERD for target stimuli over centroparietal sites, with a right hemisphere maximum that was greater for controls than patients (Fig. 7B, alpha ERD, column 2), and 2) a robust ERS for novel stimuli over mid-frontocentral sites (Fig. 7B, NVS ERS, column 3). Likewise, factor 130–1 clearly corresponds to the early ERS coinciding with the N1 sink, revealing topographies that implicate synchronized activities at the defining sink/source maxima of N1 over each hemisphere (i.e., C3-TP9 and C4-TP10) for nontarget and target stimuli, and at locations with maximum temporal N1 sink activity (e.g., T8) for

Table 3
Summary of ANOVA *F* ratios performed on temporal CSD-PCA factors at selected sites.

A	Repeated measures designs involving lateral regions over each hemisphere					
Variable	*135* N1 sink		*185* Temporal N1 sink		*505* FRN source	
	(C3/4, FC5/6)		(T7/8)		(CP1/2, C3/4, P3/4)	
	F	*p*	*F*	*p*	*F*	*p*
C	3.23	.08	9.35	.004	26.9	<.0001
G						
G × C			3.74	.06	4.13	.049
H			4.54	.04	5.64	.02
C × H			5.70	.02		
G × H						
G × C × H					5.17	.03

B	Repeated measures designs restricted to midline regions									
Variable	*185* Novelty MMN		*255* NVS		*350* P3a		*350* P3b		*505* FRN sink	
	(Fz, FCz, FC1/2, Cz)		(FCz, Cz, FC1/2)		(AFz, Fz, F3/4, FCz, FC1/2)		(Pz, P3/4, POz, CP1/2)		(AFz, Fz, FCz)	
	F	*p*	*F*	*p*	*F*	*p*	*F*	*p*	*F*	*p*
C	41.1	<.0001	53.8	<.0001	18.0	.0001			25.7	<.0001
G										
G × C	4.29	.045								

Note. C: condition (target, novel); G: group (patients, controls); H: hemisphere (left, right). Only *F* ratios with $p < .10$ are reported. For all effects, $df = 1, 38$.

novel stimuli (Fig. 7B, N1 ERS; cf. also Fig. 4B, N1). In addition to the close temporal conjunction between the tPCA and tfPCA factors associated with N1 sink and NVS, the bilateral N1 sink/source dipole pairs of grand mean CSD waveforms for targets corresponded to half-cycle sinusoids of 3.7 Hz, and the distinct sink/source sequence for novels at FCz (peaks at 190 and 285 ms) corresponded to a half-

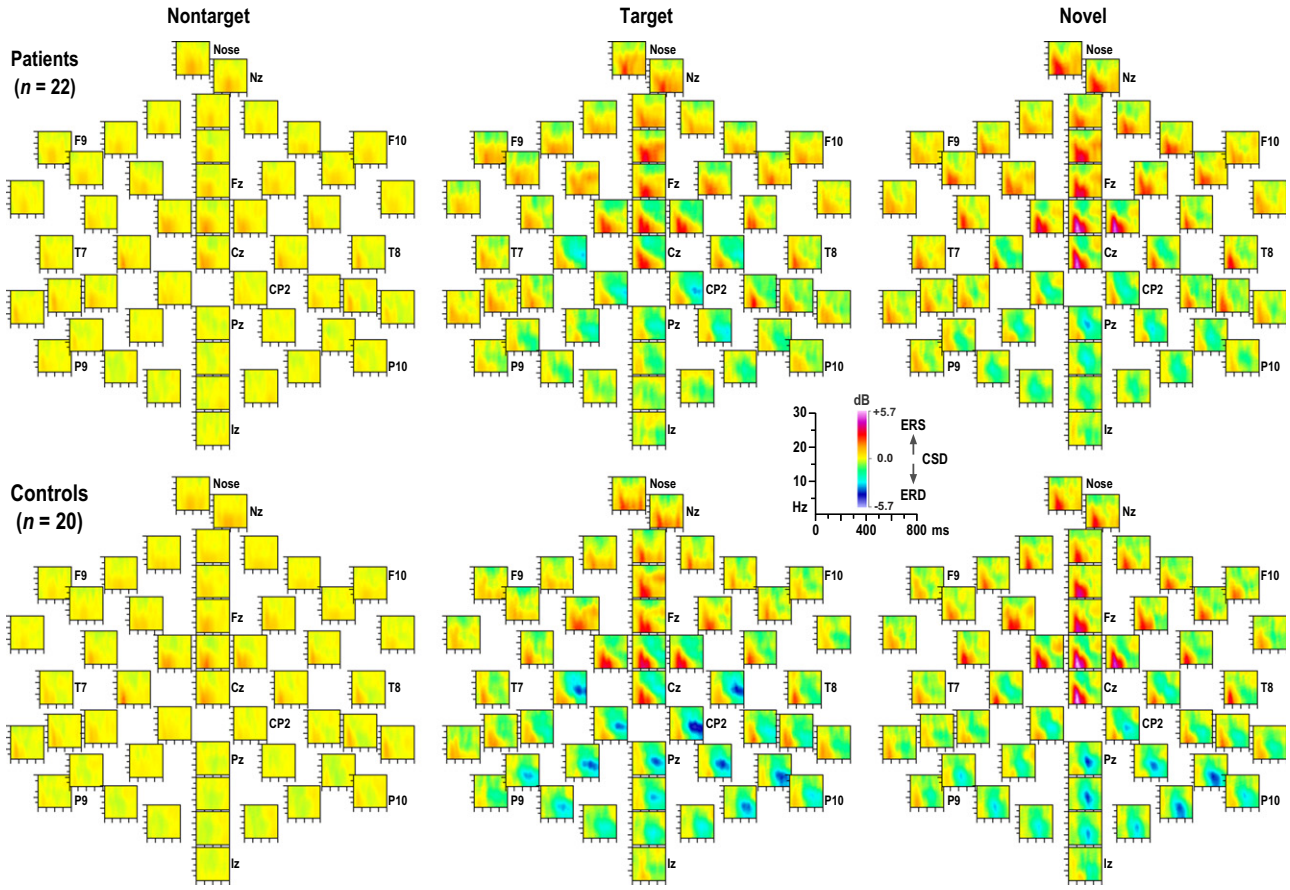

Fig. 5. Grand mean surface Laplacian (CSD) event-related spectral perturbation (ERSP) plots (−10 to 800 ms; 1 to 30 Hz) at all 49 recording sites for 22 patients (top) and 20 controls (bottom) for each condition (nontarget, target, novel). Distinct event-related synchronization (ERS) for target and novel stimuli between 100 and 400 ms is evident for both groups at anterior sites. In contrast, event-related desynchronization (ERD) is most prominent for target stimuli between 400 and 800 ms over posterior sites, and appears to be reduced for patients compared to controls.

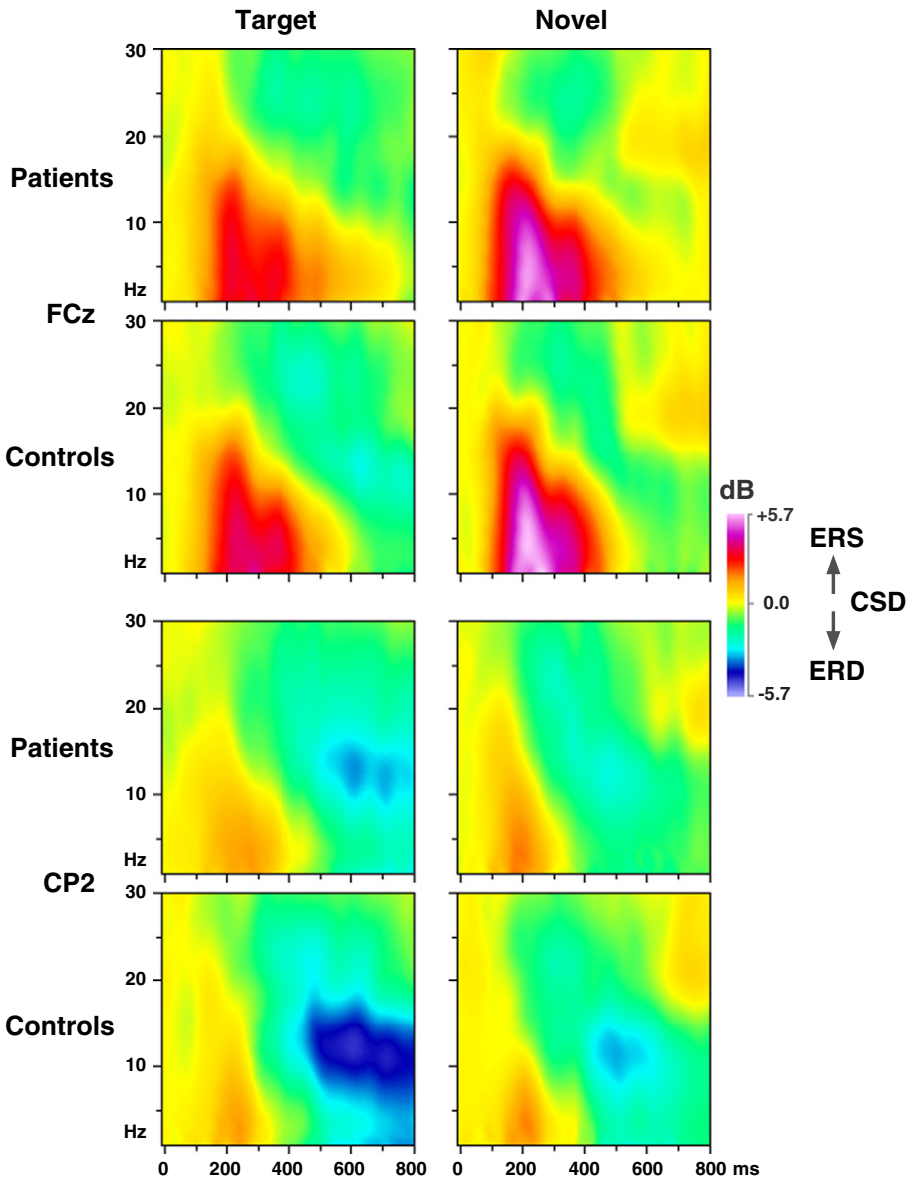

Fig. 6. CSD-ERSP plots at selected sites (FCz, CP2) for target and novel stimuli and 22 patients and 20 controls.

cycle sinusoid of 5.3 Hz, thereby falling well within the dominant delta to alpha low-frequency range captured by the two corresponding ERS factors.

Despite its loadings peak frequency, the spectral composition of the alpha ERD factor revealed considerable contributions from lower frequencies (i.e., theta and delta; Fig. 7A), indicating that the event-related desynchronization of alpha and theta oscillations around 400–800 ms covaried in this paradigm for this sample of young individuals. To corroborate the interpretation that this time–frequency component is nevertheless consistent with an alpha ERD conceptualization, an additional CSD-tfPCA solution was derived from ERSP data restricted to spectra between 8 and 30 Hz (i.e., excluding delta and theta frequencies). The resulting first five CSD-tfPCA factors were highly similar to the first five factors extracted from the original 1–30 Hz ERSP data, yielding highly correlated factor loadings ($r > .983$) and factor scores ($r > .986$) between corresponding alpha ERD and NVS ERS factors (see Supplementary Fig. S4).

The statistical analyses for the time–frequency CSD components at selected regions are summarized in Table 4. Alpha ERD at lateral centroparietal and parietal–occipital sites was significantly greater for target than novel stimuli (-0.97 ± 1.49 vs. -0.54 ± 1.12), and significantly reduced in patients compared to controls (-0.48 ± 1.21 vs. -1.06 ± 1.39). Furthermore, a highly significant main effect of hemisphere, stemming from right-greater-than-left alpha ERD (-0.90 ± 1.38 vs. -0.61 ± 1.26), was moderated by a robust interaction with group. Simple effects of hemisphere were highly significant in controls ($F[1,38] = 22.9$, $p < .0001$) but not patients ($F[1,38] < 1.0$), and simple effects of group were found for the right ($F[1,38] = 8.43$, $p = .006$) but not left hemisphere ($F[1,38] = 2.75$, $p = .11$). In contrast, no significant effects involving group or hemisphere were found for the two ERS factors, although ERS was more prominent for novel than target stimuli at mid-frontocentral sites (NVS ERS: 1.86 ± 1.28 vs. 1.16 ± 1.03) and at lateral frontocentral and temporoparietal sites (N1 ERS: 0.68 ± 1.23 vs. 0.38 ± 1.22).

To control for possible differences between groups and/or conditions in baseline power, which represents the critical variable for computing and normalizing ERS/ERD estimates (Delorme and Makeig, 2004; Makeig, 1993; Roach and Mathalon, 2008), separate repeated measures ANOVAs were performed on baseline power, which was effectively summarized by combined theta/alpha and beta activity. There were no significant group or group × condition effects in these analyses (all $F[1,38] \leq 1.57$, all $p \geq .22$).

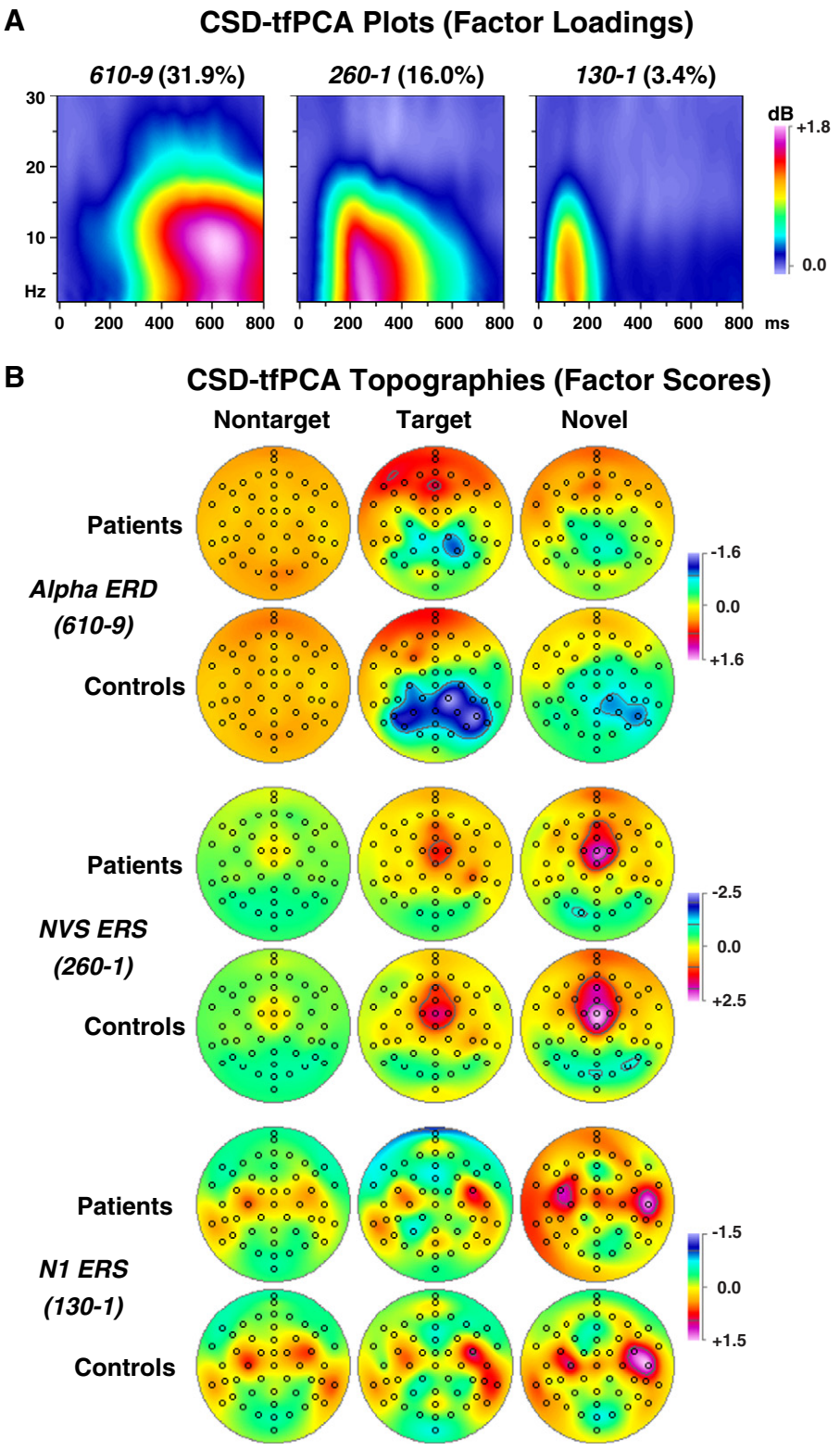

Fig. 7. (A) Factor loadings of three time–frequency PCA (tfPCA) factors (with explained variance) extracted from the time–frequency CSD matrices ($N = 42$). Factor labels reflect both peak latency [ms] and peak frequency [Hz] of the factor loadings. (B) CSD factor score topographies corresponding to alpha event-related desynchronization (ERD; factor 610–9), novelty vertex source (NVS) event-related synchronization (ERS; factor 260–1), and N1 sink ERS (factor 130–1) comparing nontarget, target and novel stimuli for 22 patients and 20 controls. All topographies are two-dimensional representations of spherical spline interpolations ($m = 2$; $\lambda = 0$) derived from the mean factors scores for each recording site.

3.2.3. Provisional observations for CHR individuals with transition to psychosis

Mean CSD waveforms and ERSP plots for the three converters are shown at selected sites in Fig. 8. Due to the extremely small subsample size, CSD waveforms were more volatile but were nevertheless characterized by robust condition effects, which included a distinct NVS for novels at Cz and a late P3b for targets with a Pz maximum (Fig. 8A). However, in striking contrast to controls and the overall sample of patients, the novelty MMN, which partially overlaps but follows N1 sink and uniquely distinguishes novel stimuli from targets

Table 4
Summary of ANOVA *F* ratios performed on time–frequency CSD-PCA factors at selected sites.

Variable	*610-9* Alpha ERD (CP1/2, CP5/6, P3/4, P7/8, PO7/8)		*260-1* NVS ERS (Fz, FCz, FC1/2, Cz)		*130-1* N1 ERS (C3/4, FC5/6, T7/8, TP9/10, P7/8)	
	F	*p*	*F*	*p*	*F*	*p*
C	4.47	.04	32.3	<.0001	6.32	.02
G	5.63	.02				
G × C						
H	14.5	.0005	–			
C × H			–			
G × H	9.26	.004	–			
G × C × H			–			

Note. C: condition (target, novel); G: group (patients, controls); H: hemisphere (left, right). Only *F* ratios with $p < .10$ are reported. For all effects, $df = 1, 38$. –: Effect not applicable.

(cf. Fig. 3, row 2), was not observed for these individuals. To highlight this observation, a shaded area was added to Fig. 8A depicting the difference from controls for novel stimuli. Fig. 9A compares novel CSDs for controls and CHR patients with and without transition to psychosis at sites where novelty MMN and NVS were most robust (i.e., at FCz and Cz; cf. Fig. 4), and Fig. 9B depicts novel-minus-nontarget difference waveforms at FCz where novelty MMN (factor 185) was maximal so as to mimic deviant-minus-standard MMN waveforms computed in passive auditory paradigms (e.g., Higuchi et al., 2013; Murphy et al., 2013). As can be seen, the three converters lacked any evidence of MMN, whereas a strong MMN response was observed between 150 and 230 ms (i.e., the typical time interval for measuring MMN) for controls and CHR patients who did not develop psychosis. To better quantify this observation, and for descriptive purposes only, a post-hoc ANOVA was computed for novelty MMN (tPCA factor *185* at mid-frontocentral sites; cf. Table 3B) with 3 converters, 19 nonconverters and 20 controls as the only between-subjects factor, which revealed a highly significant group × condition interaction ($F[2,39] = 6.73$, $p = .003$). As expected, simple effects of condition were present in controls (novels vs. targets, -1.15 ± 1.51 vs. 0.32 ± 1.02; $F[1,39] = 41.6$, $p < .0001$) and nonconverters (-0.86 ± 1.41 vs. 0.42 ± 0.82; $F[1,39] = 29.5$, $p < .0001$), but were in opposite direction and not significant in converters (1.09 ± 1.87 vs. 0.25 ± 0.70; $F[1,39] = 2.02$, $p = .16$). These parametric statistics were corroborated by non-parametric independent-samples Kruskal–Wallis tests for the novel-minus-target difference of this measure, as well as by the Approximate Degrees of Freedom (ADF) test, a robust multivariate *F* statistic for mixed designs when cell variances are heterogenous (Lix and Keselman, 1995).

CSD-ERSP plots were also less stable than the overall sample but nonetheless revealed similar condition effects, with greater ERS for target and particularly novel stimuli at mid-frontocentral sites compared to nontargets (Fig. 8B, row 1). However, alpha ERD over posterior sites was markedly reduced (Fig. 8B, row 2), even when compared with the overall sample of patients (cf. Fig. 6). A descriptive post-hoc ANOVA for alpha ERD (tfPCA factor *610–9* at lateral centroparietal and parietal–occipital sites; cf. Table 4) yielded a significant effect of group ($F[2,39] = 3.56$, $p = .04$), stemming from greater alpha ERD for controls (-1.06 ± 1.30) than nonconverters (-0.59 ± 1.22) and converters (0.21 ± 0.83). Simple effects revealed a significant difference between converters and controls ($F[1,39] = 5.77$, $p = .02$), a marginal difference between nonconverters and controls ($F[1,39] = 3.00$, $p = .09$), but no significant difference between converters and nonconverters ($F[1,39] = 2.26$, $p = .14$). This pattern of group differences was confirmed by the non-parametric ADF test, although converters also differed significantly from nonconverters in the Welch–James test statistic ($W/J[1,6.415] = 9.48$, $p = .02$). In other words, the three converters were a main contributor for the overall group difference in alpha ERD between CHR patients and controls. This absence of alpha ERD in converters becomes particularly apparent

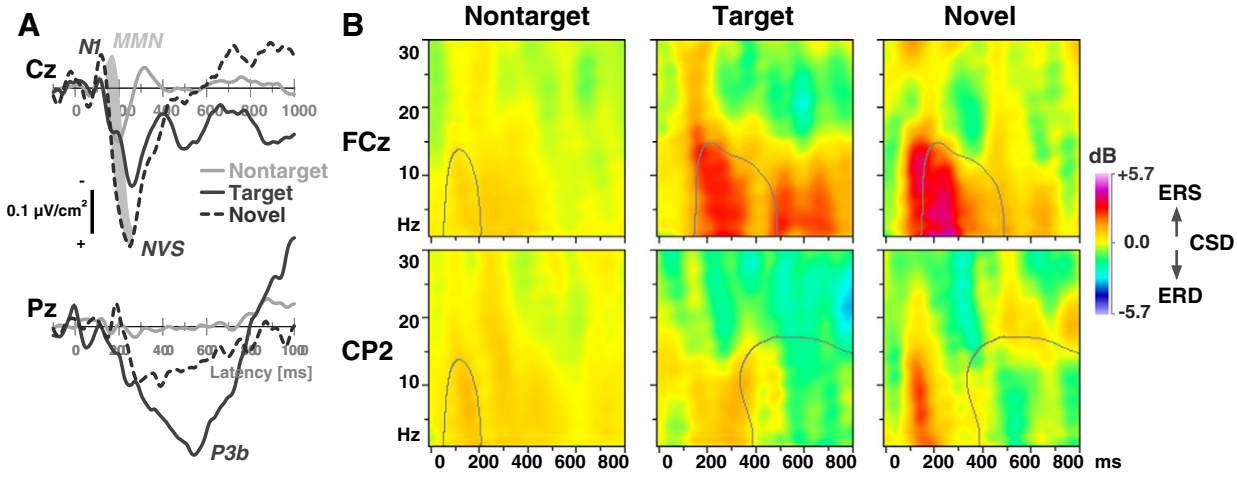

Fig. 8. Observations for CHR individuals who developed threshold psychosis within a 4-year follow-up period ($n = 3$). (A) CSD waveforms at selected midline sites (Cz, Pz) for nontarget, target and novel stimuli (scale as in Fig. 3). A prominent P3b source for targets at Pz and novelty vertex source (NVS) at Cz indicated robust condition effects, although the novelty MMN, which partially overlaps and follows N1 sink for the overall sample, is absent (grayed area). (B) CSD-ERSP plots at selected sites (FCz, CP2) for nontarget, target and novel stimuli (scale as in Fig. 6). Contour lines for nontarget stimuli depict tfPCA factor loadings (50% maximum; Fig. 7A) for N1 ERS (factor *130–1*), and NVS ERS (*260–1*) at FCz and alpha ERD (*610–9*) at CP2 for target and novel stimuli. Note that alpha ERD is virtually absent.

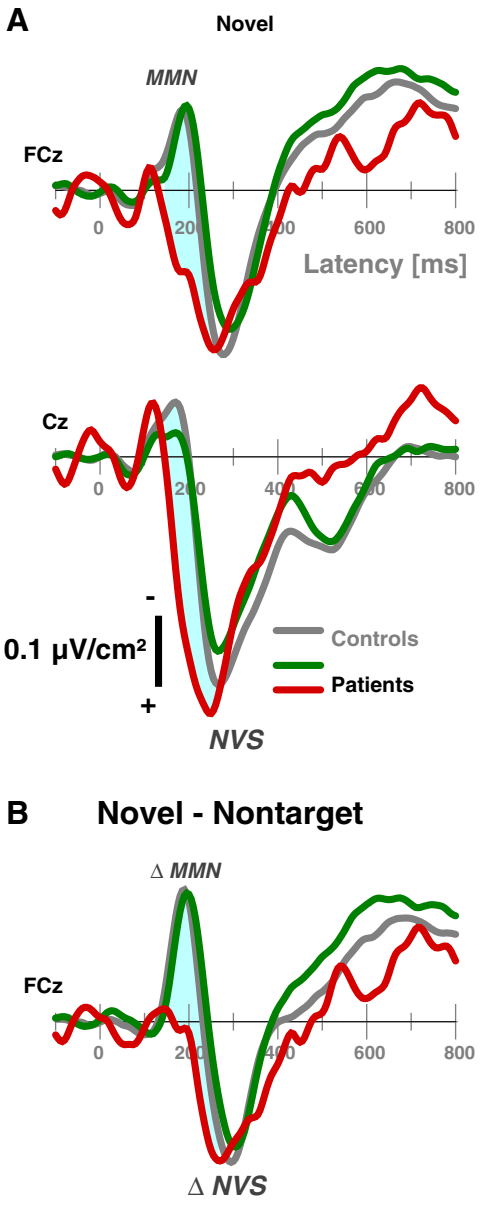

Fig. 9. (A) Novel CSD waveforms (−100 to 800 ms) at midline sites (FCz, Cz), where MMN and NVS were most prominent, for healthy controls (gray lines) and CHR patients with (red lines) and without (green lines) transition to psychosis. (B) Novel-minus-nontarget difference CSDs at FCz reveal a robust novelty MMN for controls and nonconverters, whereas ΔMMN is absent for three converters.

when using the factor loadings as a basis for comparison (contour lines in Fig. 8B). We also note that ERS as measured by factor *260–1* was mostly present in these three individuals at delta frequencies, particularly for novels, but there was clearly a less robust extension of this ERS into the alpha spectrum.

3.2.4. Correlational findings

Significant associations were found between N1 sink and N1 ERS (*135* and *130–1*, each factor pooled across condition) for both patients ($r = -0.75$, $p < 0.0001$) and controls ($r = -0.69$, $p < 0.001$), confirming that greater N1 sink was linked to increased N1 ERS. For patients, greater FRN (*505*) activity was associated with increased alpha ERD (*610–9*) for targets, as indicated by a positive correlation for the mid-frontal sink ($r = 0.55$, $p = 0.008$) and a negative correlation for the centro-parietal source ($r = -0.44$, $p = 0.04$); thus, both increases in mid-frontal sink and centroparietal sources (i.e., at either end of a sink-source dipole underlying FRN) were linked to greater alpha ERD.

Among the clinical variables considered for patients, severity of negative symptoms was correlated with reduced P3b (*350*) for targets ($r = -0.43$, $p = 0.02$) and novels ($r = -0.53$, $p = 0.005$), and reduced FRN (*505*) source at centro-parietal sites for targets was correlated with severity of general symptoms ($r = -0.47$, $p = 0.01$) and poorer global assessment of function ($r = 0.37$, $p = 0.05$). Reduced N1 ERS was associated with severity of negative symptoms (for targets, $r = -0.50$, $p = 0.008$) and poorer global assessment of function (for targets, $r = 0.46$, $p = 0.02$; for nontargets, $r = 0.47$, $p = 0.01$).

4. Discussion

CHR patients and healthy controls showed highly comparable auditory target detection performance during a novelty oddball task, and both groups had robust auditory ERPs that did not differ in morphology, amplitude, or topography. Importantly, the observed ERP/CSD component structure to frequent, target and novel stimuli in both groups directly replicates our previous findings for this paradigm using a combined CSD-PCA approach (Tenke et al., 2010). In close agreement with prior MEG findings for 17 ultra-high-risk subjects performing an auditory oddball task (Koh et al., 2011), CHR patients showed prominent abnormalities of evoked alpha activity to infrequent task-relevant target and task-irrelevant novel stimuli. The parietal alpha suppression, which prominently followed a mid-parietal target P3b in healthy controls, was markedly reduced in CHR patients, particularly over the right hemisphere. The Koh et al. (2011) study found this abnormal alpha modulation in CHR patients to be intermediate between groups of 18 healthy controls and 10 schizophrenia patients, suggesting that impaired alpha ERD may present a possible risk indicator for the development of schizophrenia. The present findings support this notion in that all three patients who later developed schizophrenia showed even more pronounced reductions of alpha ERD than the entire group of CHR patients. Koh et al. did not specify alpha ERD reductions for three individuals who made a transition to psychosis within a two-year follow-up period.

Event-related modulation of alpha has been hypothesized to reflect inhibitory cortical control processing (e.g., Uhlhaas and Singer, 2010), with alpha desynchronization indicative of the release of cortical inhibition associated with a *task-related* coordinated activation of cortical networks (Klimesch et al., 2007). In this case, the reduced alpha ERD in schizophrenia and CHR patients may reveal cognitive deficits of top-down processing (Koh et al., 2011). Interestingly, another recent MEG study (Popov et al., 2012) found that alpha desynchronization normalized in schizophrenia after cognitive training and was associated with improved verbal memory performance. While it may be objected that impairments of alpha ERD were seen for both types of infrequent events, despite being more pronounced for the active response condition, successful performance on the current task involved responding to infrequent target tones and inhibiting a response to infrequent novel sounds, thereby demanding top-down attentional control for both types of events. Notably, these oscillatory deficits were not observed with ERP measures in the time domain, which are considered complementary to ERSP measures in the time–frequency domain (e.g., Makeig et al., 2002). Fittingly, no group differences were found for two alpha/theta ERS components that were clearly linked to N1 sink and NVS activity in the time domain. Thus, the parallel analyses of ERP and ERSP measures may be particularly helpful for understanding cognitive deficits and their electrophysiological correlates in individuals at-risk for psychosis.

Low-frequency oscillations in the alpha and theta range have also been associated with default mode network (DMN) activity (e.g., Scheeringa et al., 2008; Laufs et al., 2006), and group differences in top-down control may also be related to differences in DMN activity. However, it is not likely that mere differences in

DMN activity account for the observed group differences in alpha ERD. Firstly, there were no group differences in baseline power of theta/alpha, which would be expected to directly reflect DMN activity. Secondly, alpha ERD was clearly dependent on condition, that is, it was most prominent for targets that required an active response, less present for novels that required a response inhibition, and virtually not present for nontargets. Clearly, further research is required to delineate the underlying mechanism of alpha ERD reduction in schizophrenia and CHR patients.

The close association between the time-domain FRN component and the time–frequency alpha ERD component in CHR patients is intriguing. The distinct FRN topography, consisting of its defining mid-frontal sink (negativity) accompanied by off-midline centroparietal sources (positivity), has been observed as a stimulus- as well as a response-locked CSD component across a variety of visual and auditory ERP paradigms, including tonal and phonetic oddball tasks (e.g., Kayser and Tenke, 2006a, 2006b; Kayser et al., 2010a), dichotic oddball (Tenke et al., 2008), novelty oddball (Tenke et al., 2010), and recognition memory (Kayser et al., 2007, 2010b), and interpreted as an index of ongoing motivational or action-monitoring processes. Importantly, the centroparietal source is impacted by the response requirements, being asymmetric for left or right hand responses (i.e., larger over the ipsilateral hemisphere; cf. Kayser and Tenke, 2006a; Kayser et al., 2010a) but symmetric when no manual response is required (i.e., silently counting targets). However, the press (left or right) versus no press (counting) conditions are differentiated by a superimposed hemisphere asymmetry (i.e., more negativity over the left hemisphere for press; Kayser and Tenke, 2006a; Kayser et al., 2010a). Given that this FRN topography is strikingly similar to that of the error-related negativity (ERN) observed during correct trials (e.g., Gehring and Knight, 2000; Vidal et al., 2000), the ERN has been linked to theta oscillations (Luu and Tucker, 2001; Luu et al., 2004; Bernat et al., 2005), and the present alpha ERD factor had substantial contributions from lower frequencies in the theta and delta range, it could be hypothesized that impairments in theta-modulated response monitoring may underlie or contribute to the observed reductions in alpha ERD in CHR patients.

The observed overall asymmetry in alpha ERD, as well as the lack of alpha ERD asymmetry in CHR patients, may be understood in the same context, given that the current task requirements involved unilateral responses. As most participants were right-handed, and left versus right hand responses have yielded opposite P3 source asymmetries during auditory oddball tasks (although not of comparable magnitude; e.g., Kayser and Tenke, 2006a; Kayser et al., 2010a; Tenke et al., 1998), one might speculate that asymmetric contributions of motor preparation, execution, and monitoring between 400 and 800 ms resulted in the observed alpha ERD asymmetry and its absence in CHR patients. Interestingly, Kayser et al. (2010a) found that the FRN-related source asymmetry linked to manual response versus silent count of target tones was reduced in schizophrenia. Predominant right parieto-occipital alpha ERD has also been reported for right-handed healthy adults during the anticipatory S1–S2 interval of a cued motor response task, particularly for participants with weak lateralization of sensorimotor alpha activity, suggesting distinct alpha asymmetry patterns associated with motor or attentional processes (Deiber et al., 2012). However, more research is required to clarify the mechanisms underlying these alpha ERD effects.

While the auditory ERP findings for CHR patients closely parallel those observed for olfactory stimuli in virtually the same cohort (Kayser et al., 2013), they contrast with previous reports of reduced P3a and/or P3b in CHR patients (Atkinson et al., 2012; Bramon et al., 2008; Frommann et al., 2008; van der Stelt et al., 2005; Özgürdal et al., 2008; van Tricht et al., 2010). Contrary to expectations, even the novelty vertex source (i.e., the most distinct positive component among this family of P3-like components) was not altered in CHR patients compared to healthy controls. Still, severity of negative symptoms was associated with reduced P3b, and severity of general symptoms was likewise related to the ensuing centroparietal source, that is, to ERP positivities that are typically not dissociated in conventional ERP studies (i.e., these are likely encapsulated under a broader concept of P3 or late positive complex). These findings are in line with prior evidence linking negative symptoms to P3 reductions in schizophrenia (e.g., Mathalon et al., 2000). Regarding the lack of overall P3 reductions in CHR patients, the reasons for the discordance from prior research are not clear. Apart from ample differences in ERP methodology, prior studies typically employed a standard two-tone oddball paradigm, which differed from the present three-stimulus oddball task, which includes rare, unique events likely to result in increased alertness and processing demands. However, we note that Koh et al. (2011), who used a two-tone oddball task, did not find differences between ultra-high-risk patients and healthy controls in alpha inter-trial coherence, which could be expected to be a main contributor to P3 amplitude. Importantly, the failure to observe reduced P3 amplitude in CHR patients cannot be attributed to employing CSD-PCA methods, which do not obscure or create effects that are not present in the original data (cf. Fig. 3). Clearly, more research is needed to delineate the importance of paradigmatic and other methodological aspects for uncovering electrophysiologic deficits in individuals at risk.

Although the small sample size is a limitation of the present study, with only three CHR patients who later developed psychosis, this proportion is on par with previously reported transition rates (e.g., Gee and Cannon, 2011; Simon et al., 2011). However, the observation that the CSD waveforms to novel stimuli for these three converters prominently featured the characteristic novelty vertex source (Tenke et al., 2010) but surprisingly lacked a preceding novelty MMN, is intriguing given reports of impaired duration MMN in CHR patients (Atkinson et al., 2012; Bodatsch et al., 2011; Brockhaus-Dumke et al., 2005; Higuchi et al., 2013; Hsieh et al., 2012; Jahshan et al., 2012; Murphy et al., 2013; Shaikh et al., 2012; Shin et al., 2009). While we cannot stress enough the preliminary nature of this curious observation, it nevertheless underscores the potential value of MMN as a predictor of transition to psychosis. Taken together, the present ERP and ERSP findings reveal electrophysiological abnormalities in CHR patients during an auditory oddball paradigm that warrant further research with larger samples employing longitudinal or cross-sectional designs.

Finally, the linear multivariate data-reduction approach for CSD-transformed surface potentials using unrestricted, covariance-based Varimax-PCA (e.g., Kayser and Tenke, 2003), which we have successfully applied to novelty oddball ERPs (CSD-tPCA; Tenke et al., 2010) or EEG spectra at rest (CSD-fPCA; e.g., Tenke and Kayser, 2005), has also been useful for the systematic decomposition of reference-free ERSP data (CSD-tfPCA; Tenke et al., 2012). As a logical extension of our previous CSD-PCA methods, this data-driven approach identified and effectively summarized meaningful EEG oscillations within the theta and alpha spectrum without being constrained by rigid spectral (e.g., classic frequency bands) or temporal boundaries (i.e., static time windows). As efficient summaries of the database, the neuronal generator patterns underlying these event-related oscillations can be readily depicted as topographies, thereby providing details about regional contributions to ERS or ERD not seen with conventional time–frequency EEG analysis. For example, this approach revealed scalp locations of maximum alpha/theta energy that could be directly related to CSD dipoles observed in the time domain (e.g., *N1 ERS* with *N1 sink*, *NVS ERS* with *NVS*), or be plausibly linked to known neurophysiological principles (e.g., a regional alpha/mu generator pattern). Although PCA has been employed to decompose time–frequency structure of ERP averages (e.g., Bernat et al., 2007), and EEG epochs have been CSD-transformed before employing time–frequency analysis (e.g., Cohen et al., 2009; Roberts et al., 2013), the combined CSD-PCA approach for the time–frequency analysis of EEG epochs (i.e., ERSP) is an important development. It is also noteworthy that distinct time–frequency CSD components were observed for higher frequencies (i.e., beta; cf. Supplementary Fig. S2), and, while not a focus of the present study, may offer promise for the study of

high-frequency oscillations, particularly given the negative impact of volume conduction on conventional EEG measures (e.g., Fein et al., 1988; Guevara et al., 2005; Roach and Mathalon, 2008; Schiff, 2005; Uhlhaas et al., 2008).

Supplementary data to this article can be found online at http://dx.doi.org/10.1016/j.ijpsycho.2013.12.003.

Acknowledgments

This research was supported by grants MH086125 and MH094356 from the National Institute of Mental Health (NIMH). A preliminary report of these data was presented at the 53rd Annual Meeting of the *Society of Psychophysiological Research* (*SPR*), Florence, Italy, October 2–6, 2013. We appreciate several helpful comments and suggestions received during the review process.

References

Alschuler, D.M., Tenke, C.E., Bruder, G.E., Kayser, J., 2013. Identifying electrode bridging from electrical distance distributions: a survey of publicly-available EEG data using a new method. Clin. Neurophysiol. http://dx.doi.org/10.1016/j.clinph.2013.08.024 (Oct 1. [Epub ahead of print]).

Atkinson, R.J., Michie, P.T., Schall, U., 2012. Duration mismatch negativity and P3a in first-episode psychosis and individuals at ultra-high risk of psychosis. Biol. Psychiatry 71 (2), 98–104.

Barch, D.M., Smith, E., 2008. The cognitive neuroscience of working memory: relevance to CNTRICS and schizophrenia. Biol. Psychiatry 64 (1), 11–17.

Barch, D.M., Berman, M.G., Engle, R., Jones, J.H., Jonides, J., Macdonald III, A., Nee, D.E., Redick, T.S., Sponheim, S.R., 2009. CNTRICS final task selection: working memory. Schizophr. Bull. 35 (1), 136–152.

Barch, D.M., Moore, H., Nee, D.E., Manoach, D.S., Luck, S.J., 2012. CNTRICS imaging biomarkers selection: working memory. Schizophr. Bull. 38 (1), 43–52.

Bernat, E.M., Williams, W.J., Gehring, W.J., 2005. Decomposing ERP time–frequency energy using PCA. Clin. Neurophysiol. 116 (6), 1314–1334.

Bernat, E.M., Malone, S.M., Williams, W.J., Patrick, C.J., Iacono, W.G., 2007. Decomposing delta, theta, and alpha time–frequency ERP activity from a visual oddball task using PCA. Int. J. Psychophysiol. 64 (1), 62–74.

Bodatsch, M., Ruhrmann, S., Wagner, M., Müller, R., Schultze Lutter, F., Frommann, I., Brinkmeyer, J., Gaebel, W., Maier, W., Klosterkötter, J., Brockhaus-Dumke, A., 2011. Prediction of psychosis by mismatch negativity. Biol. Psychiatry 69 (10), 959–966.

Bramon, E., McDonald, C., Croft, R.J., Landau, S., Filbey, F., Gruzelier, J.H., Sham, P.C., Frangou, S., Murray, R.M., 2005. Is the P300 wave an endophenotype for schizophrenia? A meta-analysis and a family study. Neuroimage 27 (4), 960–968.

Bramon, E., Shaikh, M., Broome, M., Lappin, J., Berge, D., Day, F., Woolley, J., Tabraham, P., Madre, M., Johns, L., Howes, O., Valmaggia, L., Perez, V., Sham, P., Murray, R.M., McGuire, P., 2008. Abnormal P300 in people with high risk of developing psychosis. Neuroimage 41 (2), 553–560.

Brockhaus-Dumke, A., Tendolkar, I., Pukrop, R., Schultze-Lutter, F., Klosterkötter, J., Ruhrmann, S., 2005. Impaired mismatch negativity generation in prodromal subjects and patients with schizophrenia. Schizophr. Res. 73 (2–3), 297–310.

Bruder, G.E., Kroppmann, C.J., Kayser, J., Stewart, J.W., McGrath, P.J., Tenke, C.E., 2009. Reduced brain responses to novel sounds in depression: P3 findings in a novelty oddball task. Psychiatry Res. 170 (2–3), 218–223.

Chapman, R.M., McCrary, J.W., 1995. EP component identification and measurement by principal components analysis. Brain Cogn. 27 (3), 288–310.

Cohen, M.X., van Gaal, S., Ridderinkhof, K.R., Lamme, V.A., 2009. Unconscious errors enhance prefrontal–occipital oscillatory synchrony. Front. Hum. Neurosci. 3, 54.

Corcoran, C.M., First, M.B., Cornblatt, B., 2010. The psychosis risk syndrome and its proposed inclusion in the DSM-V: a risk-benefit analysis. Schizophr. Res. 120 (1–3), 16–22.

Deiber, M.P., Sallard, E., Ludwig, C., Ghezzi, C., Barral, J., Ibanez, V., 2012. EEG alpha activity reflects motor preparation rather than the mode of action selection. Front. Integr. Neurosci. 6, 59.

Delorme, A., Makeig, S., 2004. EEGLAB: an open source toolbox for analysis of single-trial EEG dynamics including independent component analysis. J. Neurosci. Methods 134 (1), 9–21.

Dixon, W.J. (Ed.), 1992. BMDP Statistical Software Manual: To Accompany the 7.0 Software Release. University of California Press, Berkeley, CA.

Donchin, E., Callaway, R., Cooper, R., Desmedt, J.E., Goff, W.R., Hillyard, S.A., Sutton, S., 1977. Publication criteria for studies of evoked potentials (EP) in man. In: Desmedt, J.E. (Ed.), Progress in Clinical Neurophysiology. Attention, Voluntary Contraction and Event-Related Cerebral Potentials, 1. Karger, Basel, pp. 1–11.

Egan, M.F., Duncan, C.C., Suddath, R.L., Kirch, D.G., Mirsky, A.F., Wyatt, R.J., 1994. Event-related potential abnormalities correlate with structural brain alterations and clinical features in patients with chronic schizophrenia. Schizophr. Res. 11 (3), 259–271.

Fabiani, M., Friedman, D., 1995. Changes in brain activity patterns in aging: the novelty oddball. Psychophysiology 32 (6), 579–594.

Fabiani, M., Kazmerski, V.A., Cycowicz, Y.M., Friedman, D., 1996. Naming norms for brief environmental sounds: effects of age and dementia. Psychophysiology 33 (4), 462–475 (auditory stimuli available at http://cepl.nyspi.org/Resources/Auditory_Stimuli/auditory_stimuli.html).

Fein, G., Raz, J., Brown, F.F., Merrin, E.L., 1988. Common reference coherence data are confounded by power and phase effects. Electroencephalogr. Clin. Neurophysiol. 69 (6), 581–584.

Ford, J.M., 1999. Schizophrenia: the broken P300 and beyond. Psychophysiology 36 (6), 667–682.

Ford, J.M., White, P.M., Csernansky, J.G., Faustman, W.O., Roth, W.T., Pfefferbaum, A., 1994. ERPs in schizophrenia: effects of antipsychotic medication. Biol. Psychiatry 36 (3), 153–170.

Ford, J.M., Roach, B.J., Hoffman, R.S., Mathalon, D.H., 2008. The dependence of P300 amplitude on gamma synchrony breaks down in schizophrenia. Brain Res. 1235, 133–142.

Friedman, D., Simpson, G., Hamberger, M., 1993. Age-related changes in scalp topography to novel and target stimuli. Psychophysiology 30 (4), 383–396.

Frommann, I., Brinkmeyer, J., Ruhrmann, S., Hack, E., Brockhaus-Dumke, A., Bechdolf, A., Wölwer, W., Klosterkötter, J., Maier, W., Wagner, M., 2008. Auditory P300 in individuals clinically at risk for psychosis. Int. J. Psychophysiol. 70 (3), 192–205.

Fusar-Poli, P., Borgwardt, S., Bechdolf, A., Addington, J., Riecher-Rössler, A., Schultze-Lutter, F., Keshavan, M., Wood, S., Ruhrmann, S., Seidman, L.J., Valmaggia, L., Cannon, T., Velthorst, E., De Haan, L., Cornblatt, B., Bonoldi, I., Birchwood, M., McGlashan, T., Carpenter, W., McGorry, P., Klosterkotter, J., McGuire, P., Yung, A., 2013. The psychosis high-risk state: a comprehensive state-of-the-art review. JAMA Psychiatry 70 (1), 107–120.

Gee, D.G., Cannon, T.D., 2011. Prediction of conversion to psychosis: review and future directions. Rev. Bras. Psiquiatr. 332, 129–142.

Gehring, W.J., Knight, R.T., 2000. Prefrontal-cingulate interactions in action monitoring. Nat. Neurosci. 3 (5), 516–520.

Gruber, W.R., Klimesch, W., Sauseng, P., Doppelmayr, M., 2005. Alpha phase synchronization predicts P1 and N1 latency and amplitude size. Cereb. Cortex 15 (4), 371–377.

Guadagnoli, E., Velicer, W.F., 1988. Relation of sample size to the stability of component patterns. Psychol. Bull. 103 (2), 265–275.

Guevara, R., Velazquez, J.L., Nenadovic, V., Wennberg, R., Senjanovic, G., Dominguez, L.G., 2005. Phase synchronization measurements using electroencephalographic recordings: what can we really say about neuronal synchrony? Neuroinformatics 3 (4), 301–314.

Häfner, H., Maurer, K., Löffler, W., an der Heiden, W., Hambrecht, M., Schultze-Lutter, F., 2003. Modeling the early course of schizophrenia. Schizophr. Bull. 29 (2), 325–340.

Hay, R.A., Roach, B.J., Attygalle, S.S., Cadenhead, K., Carrion, R., Bachman, P., Johannesen, J., Duncan, E., Belger, A., Niznikiewicz, M., McCarley, R.W., Light, G., Pillay, N., Addington, J., Cannon, T., Cornblatt, B., McGlashan, T., Perkins, D., Seidman, L., Tsuang, M., Walker, E., Woods, S., Donkers, F., Consortium, N.A.P.L.S., Mathalon, D.H., 2013. Mismatch negativity abnormalities are associated with poorer functioning in youth at clinical high risk for. Biol. Psychiatry 73 (9), 272S.

Hermens, D.F., Ward, P.B., Hodge, M.A., Kaur, M., Naismith, S.L., Hickie, I.B., 2010. Impaired MMN/P3a complex in first-episode psychosis: cognitive and psychosocial associations. Prog. Neuropsychopharmacol. Biol. Psychiatry 34 (6), 822–829.

Higashima, M., Tsukada, T., Nagasawa, T., Oka, T., Okamoto, T., Okamoto, Y., Koshino, Y., 2007. Reduction in event-related alpha attenuation during performance of an auditory oddball task in schizophrenia. Int. J. Psychophysiol. 65 (2), 95–102.

Higuchi, Y., Sumiyoshi, T., Seo, T., Miyanishi, T., Kawasaki, Y., Suzuki, M., 2013. Mismatch negativity and cognitive performance for the prediction of psychosis in subjects with at-risk mental state. PLoS One 8 (1), 54080.

Hirayasu, Y., Asato, N., Ohta, H., Hokama, H., Arakaki, H., Ogura, C., 1998. Abnormalities of auditory event-related potentials in schizophrenia prior to treatment. Biol. Psychiatry 43 (4), 244–253.

Hoffmann, S., Falkenstein, M., 2012. Predictive information processing in the brain: errors and response monitoring. Int. J. Psychophysiol. 83 (2), 208–212.

Hsieh, M.H., Shan, J.C., Huang, W.L., Cheng, W.C., Chiu, M.J., Jaw, F.S., Hwu, H.G., Liu, C.C., 2012. Auditory event-related potential of subjects with suspected pre-psychotic state and first-episode psychosis. Schizophr. Res. 140 (1–3), 243–249.

Jahshan, C., Cadenhead, K.S., Rissling, A.J., Kirihara, K., Braff, D.L., Light, G.A., 2012. Automatic sensory information processing abnormalities across the illness course of schizophrenia. Psychol. Med. 42 (1), 85–97.

Javitt, D.C., Spencer, K.M., Thaker, G.K., Winterer, G., Hajos, M., 2008. Neurophysiological biomarkers for drug development in schizophrenia. Nat. Rev. Drug Discov. 7 (1), 68–83.

Jurcak, V., Tsuzuki, D., Dan, I., 2007. 10/20, 10/10, and 10/5 systems revisited: their validity as relative head-surface-based positioning systems. Neuroimage 34 (4), 1600–1611.

Kayser, J., 2009. Current source density (CSD) interpolation using spherical splines—CSD toolbox (Version 1.1). http://psychophysiology.cpmc.columbia.edu/Software/CSDtoolbox Division of Cognitive Neuroscience, New York State Psychiatric Institute.

Kayser, J., Tenke, C.E., 2003. Optimizing PCA methodology for ERP component identification and measurement: theoretical rationale and empirical evaluation. Clin. Neurophysiol. 114 (12), 2307–2325.

Kayser, J., Tenke, C.E., 2005. Trusting in or breaking with convention: towards a renaissance of principal components analysis in electrophysiology. Clin. Neurophysiol. 116 (8), 1747–1753.

Kayser, J., Tenke, C.E., 2006a. Principal components analysis of Laplacian waveforms as a generic method for identifying ERP generator patterns: I. Evaluation with auditory oddball tasks. Clin. Neurophysiol. 117 (2), 348–368.

Kayser, J., Tenke, C.E., 2006b. Principal components analysis of Laplacian waveforms as a generic method for identifying ERP generator patterns: II. Adequacy of low-density estimates. Clin. Neurophysiol. 117 (2), 369–380.

Kayser, J., Tenke, C.E., 2006c. Consensus on PCA for ERP data, and sensibility of unrestricted solutions. Clin. Neurophysiol. 117 (3), 703–707.
Kayser, J., Tenke, C.E., 2006d. Electrical distance as a reference-free measure for identifying artifacts in multichannel electroencephalogram (EEG) recordings. Psychophysiology 43, S51 (available at http://psychophysiology.cpmc.columbia.edu/mmedia/SPR2006/ElecDistArti.pdf).
Kayser, J., Tenke, C.E., 2010. In search of the Rosetta Stone for scalp EEG: converging on reference-free techniques. Clin. Neurophysiol. 121 (12), 1973–1975.
Kayser, J., Tenke, C.E., Gates, N.A., Bruder, G.E., 2007. Reference-independent ERP old/new effects of auditory and visual word recognition memory: joint extraction of stimulus- and response-locked neuronal generator patterns. Psychophysiology 44 (6), 949–967.
Kayser, J., Tenke, C.E., Gates, N.A., Kroppmann, C.J., Gil, R.B., Bruder, G.E., 2006. ERP/CSD indices of impaired verbal working memory subprocesses in schizophrenia. Psychophysiology 43 (3), 237–252.
Kayser, J., Tenke, C.E., Gil, R.B., Bruder, G.E., 2009. Stimulus- and response-locked neuronal generator patterns of auditory and visual word recognition memory in schizophrenia. Int. J. Psychophysiol. 73 (3), 186–206.
Kayser, J., Tenke, C.E., Gil, R., Bruder, G.E., 2010a. ERP generator patterns in schizophrenia during tonal and phonetic oddball tasks: effects of response hand and silent count. Clin. EEG Neurosci. 41 (4), 184–195.
Kayser, J., Tenke, C.E., Kroppmann, C.J., Fekri, S., Alschuler, D.M., Gates, N.A., Gil, R., Harkavy Friedman, J.M., Jarskog, L.F., Bruder, G.E., 2010b. Current source density (CSD) old/new effects during recognition memory for words and faces in schizophrenia and in healthy adults. Int. J. Psychophysiol. 75 (2), 194–210.
Kayser, J., Tenke, C.E., Kroppmann, C.J., Alschuler, D.M., Ben-David, S., Fekri, S., Bruder, G.E., Corcoran, C.M., 2013. Olfaction in the psychosis prodrome: electrophysiological and behavioral measures of odor detection. Int. J. Psychophysiol. 90 (2), 190–206.
Klimesch, W., Sauseng, P., Hanslmayr, S., 2007. EEG alpha oscillations: the inhibition-timing hypothesis. Brain Res. Rev. 53 (1), 63–88.
Koh, Y., Shin, K.S., Kim, J.S., Choi, J.S., Kang, D.H., Jang, J.H., Cho, K.H., O'Donnell, B.F., Chung, C.K., Kwon, J.S., 2011. An MEG study of alpha modulation in patients with schizophrenia and in subjects at high risk of developing psychosis. Schizophr. Res. 126 (1–3), 36–42.
Laufs, H., Holt, J.L., Elfont, R., Krams, M., Paul, J.S., Krakow, K., Kleinschmidt, A., 2006. Where the BOLD signal goes when alpha EEG leaves. Neuroimage 31 (4), 1408–1418.
Laurens, K.R., Kiehl, K.A., Ngan, E.T., Liddle, P.F., 2005. Attention orienting dysfunction during salient novel stimulus processing in schizophrenia. Schizophr. Res. 75 (2–3), 159–171.
Lix, L.M., Keselman, H.J., 1995. Approximate degrees of freedom tests: a unified perspective on testing for mean equality. Psychol. Bull. 117 (3), 547–560.
Luck, S.J., Mathalon, D.H., O'Donnell, B.F., Hamalainen, M.S., Spencer, K.M., Javitt, D.C., Uhlhaas, P.J., 2011. A roadmap for the development and validation of event-related potential biomarkers in schizophrenia research. Biol. Psychiatry 70 (1), 28–34.
Luu, P., Tucker, D.M., 2001. Regulating action: alternating activation of midline frontal and motor cortical networks. Clin. Neurophysiol. 112 (7), 1295–1306.
Luu, P., Tucker, D.M., Makeig, S., 2004. Frontal midline theta and the error-related negativity: neurophysiological mechanisms of action regulation. Clin. Neurophysiol. 115 (8), 1821–1835.
Makeig, S., 1993. Auditory event-related dynamics of the EEG spectrum and effects of exposure to tones. Electroencephalogr. Clin. Neurophysiol. 86 (4), 283–293.
Makeig, S., Westerfield, M., Jung, T.P., Enghoff, S., Townsend, J., Courchesne, E., Sejnowski, T.J., 2002. Dynamic brain sources of visual evoked responses. Science 295 (5555), 690–694.
Mathalon, D.H., Ford, J.M., Pfefferbaum, A., 2000. Trait and state aspects of P300 amplitude reduction in schizophrenia: a retrospective longitudinal study. Biol. Psychiatry 47 (5), 434–449.
Mathalon, D.H., Hoffman, R.E., Watson, T.D., Miller, R.M., Roach, B.J., Ford, J.M., 2010. Neurophysiological distinction between schizophrenia and schizoaffective disorder. Front. Hum. Neurosci. 3, 70.
Michie, P.T., 2001. What has MMN revealed about the auditory system in schizophrenia? Int. J. Psychophysiol. 42 (2), 177–194.
Miller, T.J., McGlashan, T.H., Woods, S.W., Stein, K., Driesen, N., Corcoran, C.M., Hoffman, R., Davidson, L., 1999. Symptom assessment in schizophrenic prodromal states. Psychiatr. Q. 70 (4), 273–287.
Miller, T.J., McGlashan, T.H., Rosen, J.L., Cadenhead, K., Cannon, T., Ventura, J., McFarlane, W., Perkins, D.O., Pearlson, G.D., Woods, S.W., 2003. Prodromal assessment with the structured interview for prodromal syndromes and the scale of prodromal symptoms: predictive validity, interrater reliability, and training to reliability. Schizophr. Bull. 29 (4), 703–715.
Murphy, J.R., Rawdon, C., Kelleher, I., Twomey, D., Markey, P.S., Cannon, M., Roche, R.A., 2013. Reduced duration mismatch negativity in adolescents with psychotic symptoms: further evidence for mismatch negativity as a possible biomarker for vulnerability to psychosis. BMC Psychiatry 13, 45.
NeuroScan, Inc., 1993. SCAN Manual II Version 3.0. Author, Herndon, VA.
NeuroScan, Inc., 2003. SCAN 4.3—Vol. II. EDIT 4.3—offline analysis of acquired data (*Document number 2203, Revision D*). Compumedics Neuroscan, El Paso, TX.
Oldfield, R.C., 1971. The assessment and analysis of handedness: the Edinburgh inventory. Neuropsychologia 9 (1), 97–113.
Özgürdal, S., Gudlowski, Y., Witthaus, H., Kawohl, W., Uhl, I., Hauser, M., Gorynia, I., Gallinat, J., Heinze, M., Heinz, A., Juckel, G., 2008. Reduction of auditory event-related P300 amplitude in subjects with at-risk mental state for schizophrenia. Schizophr. Res. 105 (1–3), 272–278.
Perrin, F., Pernier, J., Bertrand, O., Echallier, J.F., 1989. Spherical splines for scalp potential and current density mapping [Corrigenda EEG 02274, EEG Clin. Neurophysiol., 1990, 76, 565]. Electroencephalogr. Clin. Neurophysiol. 72 (2), 184–187.
Pfefferbaum, A., Ford, J.M., White, P.M., Roth, W.T., 1989. P3 in schizophrenia is affected by stimulus modality, response requirements, medication status, and negative symptoms. Arch. Gen. Psychiatry 46 (11), 1035–1044.
Pfurtscheller, G., Lopes da Silva, F.H., 1999. Event-related EEG/MEG synchronization and desynchronization: basic principles. Clin. Neurophysiol. 110 (11), 1842–1857.
Picton, T.W., Bentin, S., Berg, P., Donchin, E., Hillyard, S.A., Johnson Jr., R., Miller, G.A., Ritter, W., Ruchkin, D.S., Rugg, M.D., Taylor, M.J., 2000. Guidelines for using human event-related potentials to study cognition: recording standards and publication criteria. Psychophysiology 37 (2), 127–152.
Piskulic, D., Addington, J., Cadenhead, K.S., Cannon, T.D., Cornblatt, B.A., Heinssen, R., Perkins, D.O., Seidman, L.J., Tsuang, M.T., Walker, E.F., Woods, S.W., McGlashan, T.H., 2012. Negative symptoms in individuals at clinical high risk of psychosis. Psychiatry Res. 196 (2–3), 220–224.
Pivik, R.T., Broughton, R.J., Coppola, R., Davidson, R.J., Fox, N., Nuwer, M.R., 1993. Guidelines for the recording and quantitative analysis of electroencephalographic activity in research contexts. Psychophysiology 30 (6), 547–558.
Polich, J., 2007. Updating P300: an integrative theory of P3a and P3b. Clin. Neurophysiol. 118 (10), 2128–2148.
Popov, T., Rockstroh, B., Weisz, N., Elbert, T., Miller, G.A., 2012. Adjusting brain dynamics in schizophrenia by means of perceptual and cognitive training. PLoS One 7 (7), 39051.
Roach, B.J., Mathalon, D.H., 2008. Event-related EEG time–frequency analysis: an overview of measures and an analysis of early gamma band phase locking in schizophrenia. Schizophr. Bull. 34 (5), 907–926.
Roberts, B.M., Hsieh, L.T., Ranganath, C., 2013. Oscillatory activity during maintenance of spatial and temporal information in working memory. Neuropsychologia 51 (2), 349–357.
Salisbury, D.F., Shenton, M.E., Griggs, C.B., Bonner-Jackson, A., McCarley, R.W., 2002. Mismatch negativity in chronic schizophrenia and first-episode schizophrenia. Arch. Gen. Psychiatry 59 (8), 686–694.
Sauseng, P., Klimesch, W., Gruber, W.R., Hanslmayr, S., Freunberger, R., Doppelmayr, M., 2007. Are event-related potential components generated by phase resetting of brain oscillations? A critical discussion. Neuroscience 146 (4), 1435–1444.
Scheeringa, R., Bastiaansen, M.C., Petersson, K.M., Oostenveld, R., Norris, D.G., Hagoort, P., 2008. Frontal theta EEG activity correlates negatively with the default mode network in resting state. Int. J. Psychophysiol. 67 (3), 242–251.
Schiff, S.J., 2005. Dangerous phase. Neuroinformatics 3 (4), 315–318.
Shaikh, M., Valmaggia, L., Broome, M.R., Dutt, A., Lappin, J., Day, F., Woolley, J., Tabraham, P., Walshe, M., Johns, L., Fusar-Poli, P., Howes, O., Murray, R.M., McGuire, P., Bramon, E., 2012. Reduced mismatch negativity predates the onset of psychosis. Schizophr. Res. 134 (1), 42–48.
Shin, K.S., Kim, J.S., Kang, D.H., Koh, Y., Choi, J.S., O'Donnell, B.F., Chung, C.K., Kwon, J.S., 2009. Pre-attentive auditory processing in ultra-high-risk for schizophrenia with magnetoencephalography. Biol. Psychiatry 65 (12), 1071–1078.
Simon, A.E., Velthorst, E., Nieman, D.H., Linszen, D., de Umbricht, D., Haan, L., 2011. Ultra high-risk state for psychosis and non-transition: a systematic review. Schizophr. Res. 132 (1), 8–17.
Snodgrass, J.G., Corwin, J., 1988. Pragmatics of measuring recognition memory: applications to dementia and amnesia. J. Exp. Psychol. Gen. 117 (1), 34–50.
Spencer, K.M., Nestor, P.G., Niznikiewicz, M.A., Salisbury, D.F., Shenton, M.E., McCarley, R.W., 2003. Abnormal neural synchrony in schizophrenia. J. Neurosci. 23 (19), 7407–7411.
Spencer, K.M., Nestor, P.G., Perlmutter, R., Niznikiewicz, M.A., Klump, M.C., Frumin, M., Shenton, M.E., McCarley, R.W., 2004. Neural synchrony indexes disordered perception and cognition in schizophrenia. Proc. Natl. Acad. Sci. U. S. A. 101 (49), 17288–17293.
Tenke, C.E., Kayser, J., 2001. A convenient method for detecting electrolyte bridges in multichannel electroencephalogram and event-related potential recordings. Clin. Neurophysiol. 112 (3), 545–550.
Tenke, C.E., Kayser, J., 2005. Reference-free quantification of EEG spectra: combining current source density (CSD) and frequency principal components analysis (fPCA). Clin. Neurophysiol. 116 (12), 2826–2846.
Tenke, C.E., Kayser, J., 2012. Generator localization by current source density (CSD): implications of volume conduction and field closure at intracranial and scalp resolutions. Clin. Neurophysiol. 123 (12), 2328–2345.
Tenke, C.E., Kayser, J., Fong, R., Leite, P., Towey, J.P., Bruder, G.E., 1998. Response- and stimulus-related ERP asymmetries in a tonal oddball task: a Laplacian analysis. Brain Topogr. 10 (3), 201–210.
Tenke, C.E., Kayser, J., Shankman, S.A., Griggs, C.B., Leite, P., Stewart, J.W., Bruder, G.E., 2008. Hemispatial PCA dissociates temporal from parietal ERP generator patterns: CSD components in healthy adults and depressed patients during a dichotic oddball task. Int. J. Psychophysiol. 67 (1), 1–16.
Tenke, C.E., Kayser, J., Stewart, J.W., Bruder, G.E., 2010. Novelty P3 reductions in depression: characterization using principal components analysis (PCA) of current source density (CSD) waveforms. Psychophysiology 47 (1), 133–146.
Tenke, C.E., Kayser, J., Manna, C.G., Fekri, S., Kroppmann, C.J., Schaller, J.D., Alschuler, D.M., Stewart, J.W., McGrath, P.J., Bruder, G.E., 2011. Current source density measures of electroencephalographic alpha predict antidepressant treatment response. Biol. Psychiatry 70 (4), 388–394.
Tenke, C.E., Kayser, J., Bruder, G.E., 2012. Principal components analysis (PCA) of time–frequency (TF) measures derived from current source density (CSD) reveal a direct link between EEG alpha and the reduced novelty response in major depression. Program No. 97.04. 2012 Neuroscience Meeting Planner. Society for Neuroscience, New Orleans, LA (Online).

Turetsky, B.I., Cannon, T.D., Gur, R.E., 2000. P300 subcomponent abnormalities in schizophrenia: III. Deficits in unaffected siblings of schizophrenic probands. Biol. Psychiatry 47 (5), 380–390.
Uhlhaas, P.J., Singer, W., 2010. Abnormal neural oscillations and synchrony in schizophrenia. Nat. Rev. Neurosci. 11 (2), 100–113.
Uhlhaas, P.J., Haenschel, C., Nikolic, D., Singer, W., 2008. The role of oscillations and synchrony in cortical networks and their putative relevance for the pathophysiology of schizophrenia. Schizophr. Bull. 34 (5), 927–943.
van Boxtel, G.J.M., 1998. Computational and statistical methods for analyzing event-related potential data. Behav. Res. Methods Instrum. Comput. 30 (1), 87–102.
van der Stelt, O., Lieberman, J.A., Belger, A., 2005. Auditory P300 in high-risk, recent–onset and chronic schizophrenia. Schizophr. Res. 77 (2–3), 309–320.
van Tricht, M.J., Nieman, D.H., Koelman, J.H., van der Meer, J.N., Bour, L.J., de Haan, L., Linszen, D.H., 2010. Reduced parietal P300 amplitude is associated with an increased risk for a first psychotic episode. Biol. Psychiatry 68 (7), 642–648.
Vidal, F., Hasbroucq, T., Grapperon, J., Bonnet, M., 2000. Is the 'error negativity' specific to errors? Biol. Psychol. 51 (2–3), 109–128.
Winterer, G., Egan, M.F., Raedler, T., Sanchez, C., Jones, D.W., Coppola, R., Weinberger, D.R., 2003. P300 and genetic risk for schizophrenia. Arch. Gen. Psychiatry 60 (11), 1158–1167.